

Manuscript Number: WNS-20-2599R1

Title: Diffusion and perfusion weighted magnetic resonance imaging
methods in non-enhancing gliomas

Article Type: Literature Reviews

Keywords: Non-enhancing gliomas, Diffusion tensor imaging (DTI),
Diffusion kurtosis imaging, Perfusion imaging

Corresponding Author: Professor Harish Poptani, PhD

Corresponding Author's Institution: University of Liverpool

First Author: Hatham Alkanhal

Order of Authors: Hatham Alkanhal; Kumar Das; Harish Poptani, PhD

Abstract: Routine diagnostic magnetic resonance imaging (MRI) utilises enhancement of the tumour tissue as a marker of malignancy in intracranial gliomas. However, several high-grade tumours do not exhibit enhancement and conversely, some low-grade gliomas do demonstrate enhancement. Hence, conventional MRI has a limited role in the accurate grading of gliomas. Advanced MRI methods that evaluate the tissue microstructure and tumour haemodynamics provide a better understanding of tumour biology and promise to provide more accurate grading. These advanced MRI methods include diffusion-weighted imaging (DWI), diffusion tensor imaging (DTI), diffusion-kurtosis imaging (DKI), arterial spin labelling (ASL) imaging, dynamic-susceptibility contrast (DSC) imaging and dynamic contrast-enhanced (DCE) imaging. This review focuses on the utility of these methods for better characterisation and grading of non-enhancing gliomas and discusses how quantitative MRI data can be utilized in these settings.



Professor Harish Poptani
Department of Cellular & Molecular Physiology,
Institute of Transitional Medicine,
Nuffield Building
Crown Street, Liverpool, L69 3BX
United Kingdom
Tel: 0151 794 5444
Email: Harish.Poptani@liverpool.ac.uk

May 29, 2020

Ref: **WNS-20-2599R1**

Edward Benzel
Editor in Chief
World Neurosurgery

Dear Dr Benzel,

Thanks a lot for considering our review article for potential publication in World neurosurgery. The reviewers comments were very helpful and we have addressed them to the best of our ability. Attached is a point-by-point response to the reviewers comments, a marked copy of the revised manuscript indicating where changes have been made and a clean copy as required.

We sincerely hope that you find our revised manuscript acceptable for publication in your journal.

Please let me know if you have any questions

Sincerely,

A handwritten signature in purple ink, appearing to read 'H. Poptani'.

Harish Poptani, Ph.D.

Title: Diffusion and perfusion weighted magnetic resonance imaging methods in non-enhancing gliomas

Short Title: Diffusion and perfusion weighted MRI in non-enhancing gliomas

Type of manuscript – Review article

Authors: Hatham Alkanhal¹ MSc, Kumar Das² MB, ChB, MRCP, DMRD, FRCR, Harish Poptani¹ PhD

¹ Centre for Preclinical Imaging, University of Liverpool, Liverpool, United Kingdom.

² Department of Neuroradiology, Walton Centre NHS trust, Liverpool, United Kingdom.

*Corresponding author:

Professor Harish Poptani

Centre for Preclinical Imaging,

Nuffield Wing, Sherrington Building

Crown Street, Liverpool L69 3BX

United Kingdom

Phone: +44 151 794 5444

E-mail address: Harish.Poptani@liverpool.ac.uk

Conflict of interest:

The authors declare no conflict of interest.

Acknowledgments: Financial support to H.A. was provided by the King Saud University, Ministry of Education, Kingdom of Saudi Arabia.

Abstract:

Routine diagnostic magnetic resonance imaging (MRI) utilises enhancement of the tumour tissue as a marker of malignancy in intracranial gliomas. However, several high-grade tumours do not exhibit

enhancement and conversely, some low-grade gliomas do demonstrate enhancement. Hence, conventional MRI has a limited role in the accurate grading of gliomas. Advanced MRI methods that evaluate the tissue microstructure and tumour haemodynamics provide a better understanding of tumour biology and promise to provide more accurate grading. These advanced MRI methods include diffusion-weighted imaging (DWI), diffusion tensor imaging (DTI), diffusion-kurtosis imaging (DKI), arterial spin labelling (ASL) imaging, dynamic-susceptibility contrast (DSC) imaging and dynamic contrast-enhanced (DCE) imaging. This review focuses on the utility of these methods for better characterisation and grading of non-enhancing gliomas, as it is more difficult to accurately devise an optimal treatment strategy for these tumours in comparison to enhancing gliomas.

*Disclosure-Conflict of Interest [authors to provide own statement, .doc(x) format preferred]

[Click here to download Disclosure-Conflict of Interest \[authors to provide own statement, .doc\(x\) format preferred\]: Conflict of Interest](#)

Please see a point by point response (in blue) to the reviewer's comments

Reviewer #1:

This study described literature reviews of many studies of diffusion and perfusion weighted magnetic resonance imaging methods in non-enhanced gliomas. The authors concluded that rCBY can provide a rigorous assessment for gliomas and act as a potential imaging marker of malignancy and degree of tumor angiogenesis. This study is well organized and suggests both diffusion and perfusion imaging can promote the accuracy in diagnosis of gliomas. I think it deserve to publication of this journal.

We would like to thank for the reviewer's encouraging comments about our manuscript.

Reviewer #2:

It has been a pleasure to review your manuscript. It is a well written, organised, and interesting review. The main concern that I have about the paper is related to the conclusion. Although the abstract and the introduction are very hopeful, in the end, the conclusion gives the idea that nowadays every parameter still being useless. It maybe could be remarked or proposed how can we use them with current evidence although future studies still being necessities.

We thank the reviewer for the helpful comments. As indicated in response to the minor comments below, the conclusion has been changed appropriately

- 1- Abstract: Your work is well resumed in the abstract, however, it promised more clinical usefulness than the provided in the work "*This review focuses on the **utility of these methods for better characterisation and grading of non-enhancing gliomas, as it is more difficult to accurately devise an optimal treatment strategy for these tumours in comparison to enhancing gliomas***"

We would like to thank the reviewer for the observation and have hence rephrased the abstract accordingly. The revised text states that, "This review focuses on the utility of these methods for better characterisation and grading of non-enhancing gliomas, and discusses how quantitative MRI data can be utilized in these settings".

- 2- Introduction:

In the 4th paragraph again a clinical decision aid is promised but it is not clearly found in the paper: "The development of advanced imaging techniques, such as diffusion tensor imaging (DTI) and perfusion MRI, has enabled more sensitive tumour characterisation and grading than conventional MRI [4, 13]. These methods provide information about tumour cellularity, proliferation, disruption of white matter, tumour vascularity and vessel permeability [14, 15] and, as such, could allow for improved tumour grading [4, 16]. Therefore, the purpose of this review is to examine recent results using diffusion and perfusion methods for tumour characterisation and grading non-enhancing gliomas to aid in optimised clinical decision-making."

We believe that inclusion of diffusion and perfusion weighted imaging can aid in better diagnosis and hence clinical decision making with regards to the optimal choice of treatment strategies. We agree with the reviewer though, that we have not specifically provided a tool for the decision making and hence have deleted this phrase in the revised manuscript.

3- Discussion:

- Perfusion techniques paragraph 1: It is not said if CBF increase or decrease in LGG or HGG.

The text has been revised to indicate that CBF increases in HGG.

- Although every parameter is well explained, and supported by references, it is not clear which evidence is stronger and there are contradictory results between different papers.

As this is a review, we wanted to present an unbiased coverage of the literature. As the reviewer rightly points out, some of the data seems to be mixed with one paper describing potential utility of a particular parameter, while the other showing no value in differentiation. However, it is to be noted that the literature is not contradictory in the sense that opposing trends (higher or lower) are not reported for any particular parameter. As the trends are generally similar, we believe that the discrepancy in results are primarily due to differences in data analysis or in choice of experimental groups (including astrocytomas and oligodendrogliomas, for example) rather than the underlying insensitivity of the diffusion or perfusion imaging based parameter. We therefore recommend a standard set of imaging and analysis parameters to be used in a multi-centre prospective trial to establish the role of these parameters in non-enhancing gliomas. We have revised the text to further elaborate this point.

- At the end of diffusion studies there is an interesting resume :“ To conclude the findings of diffusion imaging, even though some evidence suggests that these methods are useful in assessing tissue microstructure and heterogeneity in brain tumours, none of the diffusion parameters in isolation have been suggested to conclusively differentiate between non-enhancing LGGs and HGGs”.
But, to sum up, what happens if we combine them? Can we do this with reliable results? Which parameters are more useful to be combined?

We would like to thank the reviewer for an excellent suggestion, and we do agree that combining the parameters are likely to provide more reliable results. As MD and FA are the most commonly used DTI parameters, we believe that combining these parameters with conventional imaging as well as perfusion imaging will be more useful. The text has been revised to add this statement

- Think about the possible utility of summarising the information in a table. It could be helpful if a table with a column for the parameters, a column for the measured aspect (cellularity, blood supply...), a column for values in HGGs, other for LGGs and other for the utility/reliability/evidence or limits of each parameter.

As suggested, we have included a table to summarize the diffusion and perfusion imaging parameters in high and low grade gliomas. The table also includes the references indicating the evidence as suggested.

- It could also be very interesting any kind of decision algorithm by using the parameters; any advice to use ones parameters instead of others, which of them are more promising, or which combinations are better when we face non-enhancing tumours in our clinical practice could be a wonderful and practical contribution.

We agree that a decision making tool/algorithm combining the various imaging parameters is highly desirable for a better diagnosis of non-enhancing gliomas in the clinical practise. This could use simplistic statistical methods such a logistic regression analyses to find the best combination of imaging parameters or use more sophisticated image analysis methods such as machine learning, artificial neural networks, artificial intelligence and deep learning. The discussion has been revised to include this aspect along with some relevant references

4- Conclusion:

It is a good conclusion that also remarks the study's limits, although I miss a conclusion with some clinical useful information as was promised in the abstract, and in the introduction.

Please see our responses above about making the changes in the abstract and introduction. Accordingly, we have revised the conclusion to state:

Both diffusion and perfusion imaging methods continue to aid in the accurate diagnosis of brain tumours; however, their role in assessing non-enhancing gliomas is still in its infancy, and the few early promising reports need to be validated in a large cohort of patients, preferably studied using a standardised, multi-central imaging trial.

5- References:

- The reference style inside the text is not the recommended from the journal as superscripts are preferred.
- The reference style is not completely correct and DOI should be included.

The references have been reformatted according to the journal style

- Reference number 60, is cited in figure 4 but not in the text.

This has been included

- There are a couple of recent papers that could be interesting for your work.
- Eur Radiol. 2020 Apr;30(4):2142-2151. doi: 10.1007/s00330-019-06548-3. Epub 2019 Dec 11.*

Diffusion- and perfusion-weighted MRI radiomics model may predict isocitrate dehydrogenase (IDH) mutation and tumor aggressiveness in diffuse lower grade glioma.

Kim M¹, Jung SY¹, Park JE², Jo Y³, Park SY⁴, Nam SJ⁵, Kim JH³, Kim HS¹.

- Asian J Neurosurg. 2019 Jan-Mar;14(1):47-51. doi: 10.4103/ajns.AJNS_191_16. Role of Diffusion and Perfusion Magnetic Resonance Imaging in Predicting the Histopathological Grade of Gliomas - A Prospective Study.*

Shoaib Y¹, Nayil K¹, Makhdoomi R², Asma A³, Ramzan A¹, Shaheen F⁴, Wani A¹.

We thank the reviewer for the suggestions, these references have been added

6- Images: Beautiful images.

We thank the reviewer for the encouraging remarks

List of abbreviations:

ADC	=	Apparent Diffusion Coefficient
ASL	=	Arterial Spin Labelling
AK	=	Axial Kurtosis
AD	=	Axial Diffusivity
CNS	=	Central Nervous System
CBF	=	Cerebral Blood Flow
CBV	=	Cerebral Blood Volume
DKI	=	Diffusion-Kurtosis Imaging
DTI	=	Diffusion Tensor Imaging
DWI	=	Diffusion-Weighted Imaging
DCE	=	Dynamic Contrast-Enhanced
DSC	=	Dynamic-Susceptibility Contrast
FLAIR	=	Fluid-Attenuated Inversion Recovery
FA	=	Fractional Anisotropy
GBCA	=	Gadolinium-Based Contrast Agents
HGG	=	High-grade Glioma
LGG	=	Low-Grade Glioma
MD	=	Mean Diffusivity
MK	=	Mean Kurtosis
MTT	=	Mean Transit Time
MRI	=	Magnetic Resonance Imaging
r	=	relative
RD	=	Radial Diffusivity
RK	=	Radial Kurtosis
WHO	=	World Health Organization

Diffusion and perfusion weighted magnetic resonance imaging methods in non-enhancing gliomas

Short title: Diffusion and perfusion weighted MRI in non-enhancing gliomas

Abstract:

Routine diagnostic magnetic resonance imaging (MRI) utilises enhancement of the tumour tissue as a marker of malignancy in intracranial gliomas. However, several high-grade tumours do not exhibit enhancement and conversely, some low-grade gliomas do demonstrate enhancement. Hence, conventional MRI has a limited role in the accurate grading of gliomas. Advanced MRI methods that evaluate the tissue microstructure and tumour haemodynamics provide a better understanding of tumour biology and promise to provide more accurate grading. These advanced MRI methods include diffusion-weighted imaging (DWI), diffusion tensor imaging (DTI), diffusion-kurtosis imaging (DKI), arterial spin labelling (ASL) imaging, dynamic-susceptibility contrast (DSC) imaging and dynamic contrast-enhanced (DCE) imaging. This review focuses on the utility of these methods for better characterisation and grading of non-enhancing gliomas and discusses how quantitative MRI data can be utilized in these settings.

Comment [PH1]: R2.1

Introduction:

Primary tumours arising in the central nervous system (CNS) are known as gliomas. The World Health Organisation (WHO) classification system is typically used to classify and grade CNS tumours based primarily on histological features of the tumour tissue, and it was updated in 2016 to include molecular markers as well ^[1, 2]. Typically, gliomas of grades I and II are considered low-grade gliomas (LGGs), while gliomas of grades III and IV are considered high-grade gliomas (HGGs) ^[3] due to the difference in treatment of low- versus high-grade gliomas. However, accurate differentiation of tumour malignancy can only be obtained through stereotactic biopsy or resected tumour tissue, which is associated with morbidity ^[4]. The risk of sampling error and the impact of the neuropathologist's experience on the outcomes are further limitations to this method ^[5].

Conventional MRI is often used for the detection and diagnosis of brain tumours ^[6]. Most clinical brain tumour MRI protocols include T1- and T2-weighted images, fluid-attenuated inversion recovery (FLAIR) images and gadolinium enhanced T1-weighted images (Figure 1). These images help determine the location, size and extent of the tumour ^[7]. Contrast enhancement using gadolinium-based contrast agents is indicative of the breakdown of the blood brain barrier (BBB). Generally, the accumulation of the contrast agent indicates whether the lesion is high-grade (presence) or low-grade (absence) ^[8, 9]. However, malignancy is also exhibited by nearly a third of non-enhancing gliomas, while enhancement is observed in certain LGGs ^[9, 10]. Hence, HGGs and LGGs cannot be definitively distinguished based on contrast enhancement alone ^[11].

In conventional MRI, LGGs appear as a homogenous mass and seldom exhibit peritumoural oedema or contrast enhancement ^[12]. In contrast, HGGs reveal heterogeneous contrast enhancement with regions of necrosis, haemorrhage, extensive peritumoural oedema and cystic regions ^[7]. These features are attributed to the cellular characteristics of HGGs, which include both grade III and IV glial tumours. Grade III tumours are characterised by mitotic and anaplastic cells and are most frequently diagnosed as anaplastic astrocytomas (AAs). On the other hand, grade IV gliomas reveal elevated vascularity and cellularity with enhanced necrotic appearance and are usually labelled as glioblastoma multiforme (GBM). Overall, the imaging features observed in LGGs and HGGs are not specific to a particular grade. In some cases, LGGs may display similar morphological features to HGGs, and the latter may present relatively benign imaging findings ^[13, 14], leading to inaccurate tumour staging. The necessity of accurate grading is exacerbated in non-enhancing gliomas because critical treatment decisions need to be made.

Surgery and chemotherapy represent the preferred treatments for HGGs, while a wait-and-watch approach is generally used to treat LGGs. Therefore, to overcome the shortcomings of conventional MRI, advanced imaging has been employed to enable quantitative analysis and improve the accuracy of diagnosis.

The development of advanced imaging techniques, such as diffusion tensor imaging (DTI) and perfusion MRI, has enabled more sensitive tumour characterisation and grading than conventional MRI ^[4, 13]. These methods provide information about tumour cellularity, proliferation, disruption of white matter, tumour vascularity and vessel permeability ^[14, 15] (summarized in Table 1) and, as such, could allow for improved tumour grading ^[4, 16]. Therefore, the purpose of this review is to examine recent results using diffusion and perfusion methods for tumour characterisation and grading non-enhancing gliomas.

Comment [PH2]: R2.3.4

Comment [PH3]: R2.2

Diffusion techniques:

Diffusion-weighted imaging (DWI) is predominantly used within neuroimaging as well as in oncological applications outside the brain. Standard DWI methods incorporate Einstein's original concept that the diffusion of water molecules follows a Gaussian (normal) distribution ^[17]. Typically, DWI measures random water molecular movement in tissue, and its derived parameter, apparent diffusion coefficient (ADC), represents direction-independent water displacement. DWI can provide information about tissue microstructure without the use of exogenous contrast agents ^[18]. Previous studies using DWI reported a strong association between ADC and cell density ^[18, 19]. It has been shown that within brain tumour tissue (high cellularity), free water motion is restricted and the measured ADC is low, whereas in normal brain tissues, the relatively lower cellularity leads to higher ADC values than those of the tumour ^[20].

The utility of ADC in characterising non-enhancing gliomas has also been investigated. One study reported that ADC values were significantly lower in HGGs compared to LGGs ^[21]. Another study observed lower ADC values in the solid portions of non-enhancing HGGs compared to LGGs ^[22], which suggested that ADC values were useful in differentiating between non-enhancing HGGs and LGGs. However, no significant differences in the ADC values of the peritumoural regions were observed in this study ^[22]. Despite these promising findings, mixed findings have also been reported with regard to the ability of ADC to differentiate LGGs from HGGs. Higher ADC values have been noted in LGGs due to their cellular morphology ^[23, 24], but overlapping ADC values between the two groups have also been reported. One study highlighted the absence of significant differences despite the higher ADC values in LGGs ^[25]. This finding was supported by a second study that reported a lack of significant differences in

ADC values between different glial tumours from either the peritumoural oedema or the solid tumour region ^[26].

The lack of significant differences in ADC values may be due to the simplistic analysis of DWI data using a mono-exponential fitting. The diffusion of water molecules in tumour tissues is much more complicated than in free water due to the complex cellular structures within the tumour microenvironment, which impacts barriers to diffusion. Consequently, the displacement probability of water in tumour tissue may substantially deviate from the conventionally used Gaussian form. Therefore, alternate diffusion models have been proposed to account for the non-Gaussian diffusion behaviour to facilitate a more comprehensive analysis of DWI data ^[17].

Diffusion kurtosis imaging (DKI) is a diffusion imaging technique that does not assume Gaussian distribution of water molecules and measures deviation from Gaussian behaviour. It has been proposed to more accurately characterise the complicated water diffusion in biological tissues. It provides additional information about tumour heterogeneity by measuring kurtosis metrics, including the mean kurtosis (MK), axial kurtosis (AK) and radial kurtosis (RK), as seen in Figure 2 ^[27, 28]. These parameters represent the mean deviation from Gaussianity, the directional deviation from Gaussianity along the axial diffusion direction and the directional deviation perpendicular to the axial diffusion direction ^[29].

A previous study assessed the contribution of DKI parameters, and demonstrated that all DKI parameters were significantly higher in HGGs when contrasted against LGGs ^[30]. The same study reported that these parameters were also significant different between grades I and II and between grades II and IV ^[30]. Tietze et al. also noted that all DKI exhibited significantly higher values in HGGs compared to LGGs ^[31]. Another study noted that the average MK value was significantly higher in the tumour cores of HGGs compared to those of LGGs ^[32]. However, another study reported that DKI variables did not differ significantly between grades II and III ^[33]. Despite these early promising findings, we are unaware of any studies specifically evaluating the utility of DKI in differentiating non-enhancing gliomas, and hence its role in these gliomas remains speculative.

The complex yet organised structure of the central nervous system (CNS), including myelinated and unmyelinated axons, cellular membrane, and the presence of proteins and intracellular organelles affect water diffusion inside the CNS. These factors could substantially impact the water diffusion pattern in the CNS, which can be broadly classified into isotropic and anisotropic diffusion ^[28]. Therefore, advanced

diffusion models using diffusion tensor imaging (DTI) have been proposed to account for diffusion directionality and the diffusion anisotropy of water in tumour tissue^[34].

DTI determines the directionality of diffusion and provides additional information on the microstructure of the brain^[27]. It involves acquisition of diffusion-weighted images in at least six diffusion gradient directions. The motion of water molecules on the X, Y and Z axes is assessed based on a calculation of three diffusion tensor eigenvalues, namely, λ_1 , λ_2 and λ_3 ^[12, 17]. The fractional anisotropy (FA), which measures the tendency of water molecules for diffusion in a particular direction, and the magnitude of diffusion (MD) represent the two most commonly studied DTI parameters. MD is mathematically analogous to the ADC value estimated by conventional DWI experiments. Furthermore, axial diffusion (AD) and radial diffusion (RD) denote the rate of diffusion along the primary diffusion axis and in the transverse direction, respectively, as displayed in Figure 3^[35, 36].

FA values have been utilised in the grading of gliomas and in demonstrating tumour infiltration in the normal brain. Various studies have reported the ability of FA to differentiate between different glioma grades^[37-39]. HGGs demonstrated significantly higher FA values than those in LGGs, with a threshold FA value of 0.188 differentiated between LGGs and HGGs^[37]. This study also reported a positive relationship between glioma cell density and FA. However, previous research has noted a negative relationship between glioma cell density and FA^[38, 40]. Another study indicated a lack of significant differences between anaplastic astrocytomas and LGGs^[41]. Utility of FA in the grading of non-enhancing gliomas has also been evaluated. A previous study suggested a cut-off value of 0.129 to separate HGGs from LGGs, with significantly lower FA values exhibited in LGGs^[16]. However, another study indicated a lack of significant differences in FA values between LGGs and HGGs from non-enhancing areas of the tumour^[42]. Yet another study reported no significant differences in FA values between grade II and III non-enhancing gliomas^[43].

MD reflects directionally averaged diffusivity of water, which is sensitive to oedema, cellularity and necrosis, [Table 1](#)^[44] and was found to be significantly lower in HGGs compared to LGGs^[25]. Another study reported that grade I gliomas exhibited significantly higher MD in comparison to grade III and IV gliomas, whilst there was a lack of difference in MD values between grade II and III gliomas^[37]. With regard to non-enhancing gliomas, Lee et al. demonstrated that even non-enhancing areas of HGGs demonstrated a significantly lower MD compared to LGGs^[42]. This result was further supported by Liu et

Comment [PH4]: R2.3.4

al. however, their findings did not reach statistical significance^[16]. On the other hand, another study reported no significant differences in MD values between grade II and III non-enhancing gliomas^[43].

Several studies have suggested that axonal integrity/degeneration can be identified through AD, while myelin damage can be identified with RD^[45, 46]. Published studies suggest that AD and RD were capable of differentiating between HGGs and LGGs^[25, 43]. Yuan et al.^[47] reported that the RD and AD values were significantly higher in LGGs than in HGGs. Another study noted that LGGs exhibited significantly higher RD and AD values when contrasted against HGGs, and this result considered differences between gliomas grades II and III and between grades II and IV^[25]. In regard to non-enhancing gliomas, one study reported no significant differences in AD and RD between grade II and III gliomas^[43].

To conclude the findings of diffusion imaging, even though some evidence suggests that these methods are useful in assessing tissue microstructure and heterogeneity in brain tumours, none of the diffusion parameters in isolation have been suggested to conclusively differentiate between non-enhancing LGGs and HGGs. However, we believe that by combining the information from the most commonly used DTI parameters, MD and FA, with conventional imaging as well as perfusion imaging (as discussed below) might aid in the accurate grading of non-enhancing gliomas. Besides having a heterogeneous structural microenvironment, brain tumours are also known to have a complex and heterogeneous vasculature, relying on angiogenesis to maintain an adequate blood supply. MRI-based perfusion imaging methods can provide information about tumour vasculature and thus may be able to aid in accurate tumour grading.

Comment [PH5]: R2.3.3

Perfusion techniques:

Perfusion MRI methods provide estimates of how well a tissue is supplied with blood. Perfusion MRI can be broadly classified into two methods: one that uses an endogenous contrast agent (water) to measure blood flow and another that uses an exogenous contrast agent, typically gadolinium-based contrast agents (GBCA), to study contrast kinetics. The first method is generally referred to as arterial spin labelling (ASL), which is a completely non-invasive MRI technique that measures blood flow by using magnetically labelled water protons in arterial blood as an endogenous tracer^[48]. The parameter most commonly derived from ASL methods is cerebral blood flow (CBF). The relative rCBF has been used to discriminate between low- and high-grade gliomas. Some studies suggest that HGGs demonstrate significantly higher rCBF values than those in LGGs^[49, 50]. Another study reported a strong correlation

Comment [PH6]: R2.3.1

between ASL-derived CBF values and dynamic susceptibility contrast (DSC)-derived CBF values in brain tumours^[51]. However, one study found that the correlation between DSC-derived rCBF and ASL-derived rCBF was weaker^[49]. To our knowledge, the use of ASL in evaluating non-enhancing gliomas has not been investigated.

Whilst ASL has the advantage of being completely non-invasive, it suffers from low signal-to-noise ratio as well as sensitivity to motion since it is a difference method in which ‘labelled’ images are subtracted from ‘control’ images^[52]. The more commonly used perfusion imaging method uses an exogenous contrast agent and can either be performed using dynamic contrast enhanced (DCE) or dynamic susceptibility contrast (DSC) enhanced imaging. DCE imaging relies on the acquisition of T1-weighted images and this method detects changes in MR signal as the contrast agent passes through the blood vessels and leaks into the interstitial space during the BBB breakdown. Hence, the images obtained through this method can be indicative of microvascular properties such as vascular permeability and flow and are indicated by the parameter K^{trans} ^[53]. DCE-MRI has been evaluated to discriminate between gliomas of different grades. The K^{trans} parameter can be used to quantify the permeability of tumour vessels, as shown in Figure 4^[54]. This study reported that the skewness of K^{trans} was superior in differentiating between grade II and grade III gliomas^[55]. In addition, significantly higher K^{trans} was reported in HGGs compared to LGGs^[54, 56–58]. It should be noted that K^{trans} reflects a combination of microvascular blood flow, vessel permeability and vessel density. These factors are correlated with the distribution of tumour vessels and abnormal permeability^[59, 60], indicating that contrast agents permeate more easily in HGGs than in LGGs. To our knowledge, DCE-MRI studies have not been reported in non-enhancing gliomas.

Comment [PH7]: R2.5.2

In DSC imaging, haemodynamic parameters are measured by studying the changes in MR intensity during the initial passage of the paramagnetic contrast agent^[28, 61]. The cerebral blood volume (CBV), cerebral blood flow (CBF) and mean transit time (MTT) constitute the main hemodynamic parameters associated with DSC-MRI. Indicative of the blood supply of a particular region of tissue at a particular moment, the CBV can be derived from the area under the fitted curve. Meanwhile, the CBV-to-MTT ratio reflects CBF. As the change in signal intensity and the gadolinium concentration is not linearly correlated, it is challenging to quantitatively measure these parameters. Hence, they are typically normalised to the contralateral white matter and the values are represented as ‘relative’ (rCBV, rCBF and rMTT), as depicted in Figure 5^[62, 63]. DSC has been shown to differentiate between LGGs and HGGs. Some studies have reported that rCBV values aid in differentiation between various glioma grades by recognising histopathological features, including vascularisation and the degree of angiogenesis, Table 1^[64, 65]. The

Comment [PH8]: R2.3.4

rCBV values of LGGs were negligible or very low, indicating minimal vascularisation when contrasted against HGGs. Anaplastic astrocytomas demonstrated higher rCBV values compared to LGGs, but these values were lower than in GBMs, the latter representing gliomas with the greatest level of hypervascularisation. Several studies have also reported variation in the degree of vascularisation of LGGs and HGGs [16, 66-69]. Despite the range of rCBV values reported in the literature amongst various types of gliomas, the commonality was the observation of higher rCBV in gliomas, which was likely due to the associated micro-vascular density noted in each grade. It is important to realise that gliomas constitute a heterogeneous range of tumours and overlap in rCBV values should be expected. For example, even low-grade oligodendrogliomas have been noted to have higher angiogenesis, which correlated with higher rCBV values than typically reported in HGGs [16, 70, 71].

Utilising DSC derived parameters to differentiate between non-enhancing LGGs and HGGs has led to ambiguous findings. Liu et al. reported a lack of significant differences in rCBV ratios between LGGs and HGGs [16], whereas, Fan et al. noted significantly higher rCBV values in non-enhancing areas of HGGs than in LGGs [72]. The latter study also noted significant variation in rCBV values in peritumoural regions [72]. This was supported by a study that reported statistically higher rCBV_{max} ratios for grade III astrocytomas compared to grade I or grade II astrocytomas [11]. However, previous studies also demonstrated no significant differences in rCBV_{max} between grade II and III non-enhancing gliomas [43, 73].

With regard to the utility of MTT and DSC-derived rCBF values in non-enhancing gliomas, one study reported significant differences in rCBF and rMTT between grade II and GBM [43]. However, in the same study, no significant differences in rCBF and rMTT were noted between grade II and grade III non-enhancing gliomas [43]. Another study reported significant differences in rCBF values between these two grades of gliomas [74]. This finding was further supported by a study that reported higher rCBF values associated with grades of gliomas, with significant variation identified between LGGs and HGGs [67].

Despite the observed variability in results, which may in part be due to a small sample size, methodological differences or the inclusion of different histological sub-types of gliomas, it is generally accepted that rCBV provides a rigorous means of assessing gliomas, thereby allowing it to act as a potential imaging marker of malignancy and degree of tumour angiogenesis, at least for enhancing tumours.

We acknowledge that the current literature, with mixed results about the utility of diffusion and perfusion imaging in non-enhancing gliomas is still emerging, but we believe that the data is not contradictory in the sense that opposing values (higher or lower between HGG and LGG) are not reported for any particular parameter. As the trends are generally similar between different studies, we believe that the apparent discrepancy is primarily due to differences in data analysis or in choice of experimental groups (including astrocytomas and oligodendrogliomas together, for example) rather than the underlying insensitivity of the diffusion or perfusion imaging based parameter. We therefore recommend a standard set of imaging and analysis parameters evaluated in a homogenous histological subgroup, to be used in a multi-centre prospective trial to establish the role of these parameters in non-enhancing gliomas. In addition, a decision-making tool/algorithm combining the various imaging parameters is highly desirable for a better diagnosis of non-enhancing gliomas in the clinical practise. This could use simplistic statistical methods such a logistic regression analyses to find the best combination of imaging parameters or use more sophisticated image analysis methods such as machine learning, artificial neural networks, artificial intelligence or deep learning methods ^[75-77].

Comment [PH9]: R2.3.2

Comment [PH10]: R2.3.5

Conclusion:

Both diffusion and perfusion imaging methods continue to aid in the accurate diagnosis of brain tumours; however, their role in assessing non-enhancing gliomas is still in its infancy, and the few early promising reports need to be validated in a large cohort of patients, preferably studied using a standardised, multi-center imaging trial.

Comment [PH11]: R2.4

References:

Comment [PH12]: R2.5

1. Louis, D.N., et al., *The 2007 WHO classification of tumours of the central nervous system*. Acta Neuropathologica, 2007. 114(5): p. 547-547 DOI: 10.1007/s00401-007-0278-6.
2. Raizer, J. and A. Parsa, *Current understanding and treatment of gliomas*. Vol. 163. 2015: Springer.
3. Wesseling, P. and D. Capper, *WHO 2016 Classification of gliomas*. Neuropathol Appl Neurobiol, 2018. 44(2): p. 139-150 DOI: 10.1111/nan.12432.
4. Guzman-De-Villoria, J.A., et al., *Added value of advanced over conventional magnetic resonance imaging in grading gliomas and other primary brain tumors*. Cancer Imaging, 2014. 14(1): p. 35 DOI: 10.1186/s40644-014-0035-8.
5. Muragaki, Y., et al., *Low-grade glioma on stereotactic biopsy: how often is the diagnosis accurate?* Min-minimally invasive Neurosurgery, 2008. 51(05): p. 275-279 DOI: 10.1055/s-0028-1082322
6. Herberholz, J., et al., *Non-invasive imaging of neuroanatomical structures and neural activation with high-resolution MRI*. Front Behav Neurosci, 2011. 5: p. 16 DOI: 10.3389/fnbeh.2011.00016.
7. Villanueva-Meyer, J.E., M.C. Mabray, and S. Cha, *Current Clinical Brain Tumor Imaging*. Neurosurgery, 2017. 81(3): p. 397-415 DOI: 10.1093/neuros/nyx103.
8. Mabray, M.C., R.F. Barajas, Jr., and S. Cha, *Modern brain tumor imaging*. Brain Tumor Res Treat, 2015. 3(1): p. 8-23 DOI: 10.14791/btrt.2015.3.1.8.
9. Scott, J.N., et al., *How often are nonenhancing supratentorial gliomas malignant? A population study*, Neurology, 2002. 59(6): p. 947-949 DOI: 10.1212/WNL.59.6.947.
10. Upadhyay, N. and A.D. Waldman, *Conventional MRI evaluation of gliomas*. Br J Radiol, 2011. 84 Spec No 2: p. S107-11 DOI: 10.1259/bjr/65711810.
11. Morita, N., et al., *Dynamic susceptibility contrast perfusion weighted imaging in grading of nonenhancing astrocytomas*. Journal of Magnetic Resonance Imaging, 2010. 32(4), pp.803-808 DOI: 10.1002/jmri.22324.
12. Guillemin, R., et al., *Low-grade gliomas: the challenges of imaging*. Diagn Interv Imaging, 2014. 95(10): p. 957-63 DOI: 10.1016/j.diii.2014.07.005.
13. Drake-Perez, M., et al., *Clinical applications of diffusion weighted imaging in neuroradiology*. Insights Imaging, 2018. 9(4): p. 535-547 DOI: 10.1007/s13244-018-0624-3.
14. Young, G.S., *Advanced MRI of adult brain tumors*. Neurol Clin, 2007. 25(4): p. 947-73, viii DOI: 10.1016/j.ncl.2007.07.010.
15. Saini, J., et al., *Comparative evaluation of cerebral gliomas using rCBV measurements during sequential acquisition of T1-perfusion and T2*-perfusion MRI*. PLoS One, 2019. 14(4): p. e0215400. DOI: 10.1371/journal.pone.0215400.
16. Liu, X., et al., *MR diffusion tensor and perfusion-weighted imaging in preoperative grading of supratentorial nonenhancing gliomas*. Neuro Oncol, 2011. 13(4): p. 447-55 DOI: 10.1093/neuonc/noq197.
17. Yuan, J., et al., *Non-Gaussian Analysis of Diffusion Weighted Imaging in Head and Neck at 3T: A Pilot Study in Patients with Nasopharyngeal Carcinoma*. PLoS One, 2014. 9(1): p. e87024. DOI: 10.1371/journal.pone.0087024.
18. Harkins, K.D., et al., *Assessment of the effects of cellular tissue properties on ADC measurements by numerical simulation of water diffusion*. Magn Reson Med, 2009. 62(6): p. 1414-22 DOI: 10.1002/mrm.22155.
19. Surov, A., H.J. Meyer, and A. Wienke, *Correlation between apparent diffusion coefficient (ADC) and cellularity is different in several tumors: a meta-analysis*. Oncotarget. 2017. 8(35): p. 59492-59499 DOI:10.18632/oncotarget.17752.

20. Bulakbasi, N. and Y. Paksoy, *Advanced imaging in adult diffusely infiltrating low-grade gliomas*. Insights Imaging, 2019. 10(1): p. 122 DOI: 10.1186/s13244-019-0793-8.
21. Hu, Y.-C., et al., *Comparison between ultra-high and conventional mono b-value DWI for preoperative glioma grading*. Oncotarget, 2017. 8(23): p. 37884-37895 DOI:10.18632/oncotarget.14180.
22. Fan, G.G., et al., *Usefulness of diffusion/perfusion-weighted MRI in patients with non-enhancing supratentorial brain gliomas: a valuable tool to predict tumour grading?* Br J Radiol, 2006. 79(944): p. 652-8 DOI: 10.1259/bjr/25349497.
23. Yamasaki, F., et al., *Apparent diffusion coefficient of human brain tumors at MR imaging*. Radiology, 2005. 235(3): p. 985-991 DOI: 10.1148/radiol.2353031338.
24. Svolos, P., et al., *Investigating brain tumor differentiation with diffusion and perfusion metrics at 3T MRI using pattern recognition techniques*. Magn Reson Imaging, 2013. 31(9): p. 1567-77 DOI: 10.1016/j.mri.2013.06.010.
25. Server, A., et al., *Analysis of diffusion tensor imaging metrics for gliomas grading at 3 T*. Eur J Radiol, 2014. 83(3): p. e156-65 DOI: 10.1016/j.ejrad.2013.12.023.
26. Rizzo, L., et al., *Role of diffusion- and perfusion-weighted MR imaging for brain tumour characterisation*. Radiol Med, 2009. 114(4): p. 645-59 DOI: 10.1007/s11547-009-0401-y.
27. Steven, A.J., J. Zhuo, and E.R. Melhem, *Diffusion kurtosis imaging: an emerging technique for evaluating the microstructural environment of the brain*. AJR Am J Roentgenol, 2014. 202(1): p. W26-33 DOI: 10.2214/AJR.13.11365.
28. Arab, A., et al., *Principles of diffusion kurtosis imaging and its role in early diagnosis of neurodegenerative disorders*. Brain Res Bull, 2018. 139: p. 91-98 DOI: 10.1016/j.brainresbull.2018.01.015.
29. Wang, S., et al., *Empirical comparison of diffusion kurtosis imaging and diffusion basis spectrum imaging using the same acquisition in healthy young adults*. Frontiers in neurology, 2017. 8: p. 118 DOI:10.3389/fneur.2017.00118.
30. Andersson, J.L.R. and S.N. Sotiropoulos, *An integrated approach to correction for off-resonance effects and subject movement in diffusion MR imaging*. Neuroimage, 2016. 125: p. 1063-1078 DOI: 10.1016/j.neuroimage.2015.10.019.
31. Tietze, A., et al., *Mean Diffusional Kurtosis in Patients with Glioma: Initial Results with a Fast Imaging Method in a Clinical Setting*. AJNR Am J Neuroradiol, 2015. 36(8): p. 1472-8 DOI: 10.3174/ajnr.A4311.
32. Raab, P., et al., *Cerebral gliomas: diffusional kurtosis imaging analysis of microstructural differences*. Radiology, 2010. 254(3): p. 876-81 DOI: 10.1148/radiol.09090819.
33. Delgado, A.F., et al., *Diffusion Kurtosis Imaging of Gliomas Grades II and III - A Study of Perilesional Tumor Infiltration, Tumor Grades and Subtypes at Clinical Presentation*. Radiol Oncol, 2017. 51(2): p. 121-129 DOI: 10.1515/raon-2017-0010.
34. Dubey, A., R. Kataria, and V.D. Sinha, *Role of Diffusion Tensor Imaging in Brain Tumor Surgery*. Asian J Neurosurg, 2018. 13(2): p. 302-306 DOI: 10.4103/ajns.AJNS_226_16.
35. Zeestraten, E.A., et al., *Application of Diffusion Tensor Imaging Parameters to Detect Change in Longitudinal Studies in Cerebral Small Vessel Disease*. PLoS One, 2016. 11(1): p. e0147836 DOI: 10.1371/journal.pone.0147836.
36. Abdullah, K.G., et al., *Use of diffusion tensor imaging in glioma resection*. Neurosurgical focus, 2013. 34(4), p.E1 DOI: 10.3171/2013.1.FOCUS12412.
37. Inoue, T., et al., *Diffusion tensor imaging for preoperative evaluation of tumor grade in gliomas*. Clin Neurol Neurosurg, 2005. 107(3): p. 174-80 DOI: 10.1016/j.clineuro.2004.06.011.
38. El-Serougy, L., et al., *Assessment of diffusion tensor imaging metrics in differentiating low-grade from high-grade gliomas*. Neuroradiol J, 2016. 29(5): p. 400-7 DOI: 10.1177/1971400916665382.

39. Jiang, R., et al., *The value of diffusion tensor imaging in differentiating high-grade gliomas from brain metastases: a systematic review and meta-analysis*. PLoS One, 2014. 9(11): p. e112550 DOI: 10.1371/journal.pone.0112550.
40. Stadlbauer, A., et al., *Gliomas: histopathologic evaluation of changes in directionality and magnitude of water diffusion at diffusion-tensor MR imaging*. Radiology, 2006. 240(3): p. 803-810 DOI: 10.1148/radiol.2403050937.
41. Goebell, E., et al., *Low-grade and anaplastic gliomas: differences in architecture evaluated with diffusion-tensor MR imaging*. Radiology, 2006. 239(1): p. 217-22 DOI: 10.1148/radiol.2383050059.
42. Lee, H.Y., et al., *Diffusion-tensor imaging for glioma grading at 3-T magnetic resonance imaging: analysis of fractional anisotropy and mean diffusivity*. Journal of computer assisted tomography, 2008. 32(2): p. 298-303 DOI: 10.1097/RCT.0b013e318076b44d.
43. Alkanhal, H., et al., *Evaluating the role of Diffusion Tensor Imaging and Dynamic Susceptibility Contrast perfusion imaging in the diagnosis of non-enhancing brain tumours*. 2020, University of liverpool: Liverpool.
44. Alexander, A.L., et al., *Diffusion tensor imaging of the brain*. Neurotherapeutics, 2007. 4(3): p. 316-29 DOI: 10.1016/j.nurt.2007.05.011.
45. Zhu, F.P., et al., *Clinical application of motor pathway mapping using diffusion tensor imaging tractography and intraoperative direct subcortical stimulation in cerebral glioma surgery: a prospective cohort study*. Neurosurgery, 2012. 71(6): p. 1170-83; discussion 1183-4 DOI: 10.1227/NEU.0b013e318271bc61.
46. Rajagopalan, V., et al., *A Basic Introduction to Diffusion Tensor Imaging Mathematics and Image Processing Steps*. Brain Disord Ther, 2017. 6(229): p. 2 DOI: 10.4172/2168-975X.1000229.
47. Yuan, W., et al., *Characterization of abnormal diffusion properties of supratentorial brain tumors: a preliminary diffusion tensor imaging study*. J Neurosurg Pediatr, 2008. 1(4): p. 263-9 DOI: 10.3171/PED/2008/1/4/263.
48. Haller, S., et al., *Arterial Spin Labeling Perfusion of the Brain: Emerging Clinical Applications*. Radiology, 2016. 281(2): p. 337-356 DOI: 10.1148/radiol.2016150789.
49. Cebeci, H., et al., *Assesment of perfusion in glial tumors with arterial spin labeling; comparison with dynamic susceptibility contrast method*. European Journal of Radiology, 2014. 83(10): p. 1914-1919 DOI: 10.1016/j.ejrad.2014.07.002.
50. Kong, L., et al., *A meta-analysis of arterial spin labelling perfusion values for the prediction of glioma grade*. Clinical Radiology, 2017. 72(3): p. 255-261 DOI: 10.1016/j.crad.2016.10.016.
51. Arisawa, A., et al., *Comparative study of pulsed-continuous arterial spin labeling and dynamic susceptibility contrast imaging by histogram analysis in evaluation of glial tumors*. Neuroradiology, 2018. 60(6): p. 599-608 DOI: 10.1007/s00234-018-2024-2.
52. Ferré, J.C., et al., *Arterial spin labeling (ASL) perfusion: Techniques and clinical use*. Diagnostic and Interventional Imaging, 2013. 94(12): p. 1211-1223 DOI: 10.1016/j.diii.2013.06.010.
53. Pope, W.B. and G. Brandal, *Conventional and advanced magnetic resonance imaging in patients with high-grade glioma*. Q J Nucl Med Mol Imaging, 2018. 62(3): p. 239 -253 DOI:10.23736/S1824-4785.18.03086-8.
54. Lacerda, S. and M. Law, *Magnetic resonance perfusion and permeability imaging in brain tumors*. Neuroimaging Clin N Am, 2009. 19(4): p. 527-57 DOI: 10.1016/j.nic.2009.08.007.
55. Falk, A., et al., *Discrimination between glioma grades II and III in suspected low-grade gliomas using dynamic contrast-enhanced and dynamic susceptibility contrast perfusion MR imaging: a histogram analysis approach*. Neuroradiology, 2014. 56(12): p. 1031-8 DOI: 10.1007/s00234-014-1426-z.
56. Zhao, J., et al., *Quantitative Evaluation of Diffusion and Dynamic Contrast-Enhanced MR in Tumor Parenchyma and Peritumoral Area for Distinction of Brain Tumors*. PLoS ONE, 2015. 10(9): p. 1-15 DOI: 10.1371/journal.pone.0138573.

57. Thompson, G., et al., *Imaging of brain tumors: perfusion/permeability*. Neuroimaging Clin N Am, 2010. 20(3): p. 337-53 DOI: 10.1016/j.nic.2010.04.008.
58. Jia, Z., et al., *Quantitative analysis of neovascular permeability in glioma by dynamic contrast-enhanced MR imaging*. J Clin Neurosci, 2012. 19(6): p. 820-3 DOI: 10.1016/j.jocn.2011.08.030.
59. Bulnes, S., J. Bilbao, and J.V. Lafuente, *Microvascular adaptive changes in experimental endogenous brain gliomas*. Histol Histopathol, 2009. 24(6): p. 693-706 DOI: 10.14670/HH-24.693.
60. Morabito, R., et al., *DCE and DSC perfusion MRI diagnostic accuracy in the follow-up of primary and metastatic intra-axial brain tumors treated by radiosurgery with cyberknife*. Radiat Oncol, 2019. 14(1): p. 65 DOI: 10.1186/s13014-019-1271-7.
61. Calamante, F., *Perfusion magnetic resonance imaging quantification in the brain*, in *Visualization Techniques*. Korean J Radiol, 2014. 15(5): p. 554-577. DOI:10.3348/kjr.2014.15.5.554.
62. Calamante, F., *Perfusion MRI using dynamic-susceptibility contrast MRI: quantification issues in patient studies*. Topics in Magnetic Resonance Imaging, 2010. 21(2): p. 75-85 DOI: 10.1097/RMR.0b013e31821e53f5.
63. Price, S.J., *The role of advanced MR imaging in understanding brain tumour pathology*. Br J Neurosurg, 2007. 21(6): p. 562-75 DOI: 10.1080/02688690701700935.
64. Essig, M., et al., *Perfusion MRI: the five most frequently asked technical questions*. American Journal of Roentgenology, 2013. 200(1): p. 24-34 DOI:10.2214/AJR.12.9543.
65. Fussell, D. and R.J. Young, *Role of MRI perfusion in improving the treatment of brain tumors*. Imaging in Medicine, 2013. 5(5): p. 407-426 DOI: 10.2217/iim.13.50.
66. Geneidi, E.A.S.H., et al., *Potential role of quantitative MRI assessment in differentiating high from low-grade gliomas*. The Egyptian Journal of Radiology and Nuclear Medicine, 2016. 47(1): p. 243-253 DOI: 10.1016/j.ejrm.2015.11.005.
67. Ma, H., et al., *Three-dimensional arterial spin labeling imaging and dynamic susceptibility contrast perfusion-weighted imaging value in diagnosing glioma grade prior to surgery*. Exp Ther Med, 2017. 13(6): p. 2691-2698 DOI: 10.3892/etm.2017.4370.
68. Xu, W., et al., *The performance of MR perfusion-weighted imaging for the differentiation of high-grade glioma from primary central nervous system lymphoma: A systematic review and meta-analysis*. PLoS One, 2017. 12(3): p. e0173430 DOI: 10.1371/journal.pone.0173430.
69. Abrigo, J.M., et al., *Magnetic resonance perfusion for differentiating low-grade from high-grade gliomas at first presentation*. Cochrane Database Syst Rev, 2018. 1(1): p. CD011551 DOI: 10.1002/14651858.CD011551.pub2.
70. Cha, S., et al., *Differentiation of low-grade oligodendrogliomas from low-grade astrocytomas by using quantitative blood-volume measurements derived from dynamic susceptibility contrast-enhanced MR imaging*. American journal of neuroradiology, 2005. 26(2): p. 266-273 PMID: 15709123.
71. Xu, M., et al., *Comparison of magnetic resonance spectroscopy and perfusion-weighted imaging in presurgical grading of oligodendroglial tumors*. Neurosurgery, 2005. 56(5): p. 919-26 PMID: 15854239.
72. Fan, G.G., et al., *Usefulness of diffusion/perfusion-weighted MRI in patients with non-enhancing supratentorial brain gliomas: a valuable tool to predict tumour grading?*. BRIT INSTITUTE OF RADIOLOGY, 2006. 79(944): p. 652-8 DOI: 10.1259/bjr/25349497.
73. Sahin, N., et al., *Advanced MR imaging techniques in the evaluation of nonenhancing gliomas: perfusion-weighted imaging compared with proton magnetic resonance spectroscopy and tumor grade*. Neuroradiol J, 2013. 26(5): p. 531-41 DOI: 10.1177/197140091302600506.
74. Hakyemez, B., et al., *High-grade and low-grade gliomas: differentiation by using perfusion MR imaging*. Clin Radiol, 2005. 60(4): p. 493-502 DOI: 10.1016/j.crad.2004.09.009.

75. Booth, T. et al., *Machine learning and glioma imaging biomarkers*. Clinical radiology, 2019. 75(1), p. 20-32 DOI: 10.1016/j.crad.2019.07.001.
76. Kim M, Jung SY, Park JE, et al., *Diffusion- and perfusion-weighted MRI radiomics model may predict isocitrate dehydrogenase (IDH) mutation and tumor aggressiveness in diffuse lower grade glioma*. Eur Radiol, 2020. 30(4). P. 2142-2151 DOI:10.1007/s00330-019-06548-3.
77. Shoaib Y., et al., *Role of Diffusion and Perfusion Magnetic Resonance Imaging in Predicting the Histopathological Grade of Gliomas - A Prospective Study*. Asian J Neurosurg, 2019. 14(1): p. 47-51. DOI: 10.4103/ajns.AJNS_191_16.

Figure legends:

Figure 1: MR images of a patient with a grade III anaplastic astrocytoma who underwent conventional diagnostic MRI. (A) axial T1-weighted pre-contrast, (B) T2 and (C) T1 post-contrast images. No contrast agent enhancement was observed in this patient.

Figure 2: Representative diffusion kurtosis images from a patient with an oligodendroglioma grade II in the right frontal lobe. (A) axial kurtosis, (B) axial diffusivity and (C) radial kurtosis [33].

Figure 3: Representative DTI-derived parametric maps from a patient with a grade II astrocytoma. In FA, the white matter (WM) appears hyper-intense, while the cerebrospinal fluid (CSF) and the tumour appear hypo-intense. In contrast, in MD, AD and RD, the CSF and the tumour are hyper-intense, while the WM appears hypo-intense.

Figure 4: Follow-up MRI of a left frontal primary GBM treated by surgery and stereotactic radiosurgery (SRS). (A) axial contrast-enhanced T1-weighted image demonstrating the enhancing tumour in the frontal lobe, (B) The relative cerebral blood volume rCBV colorimetric map overlaid on the MR image and (C) pixel-by-pixel K^{trans} colorimetric map showing heterogeneous K^{trans} values from the tumour [60].

Figure 5: DSC maps showing the tumour (arrow) from a patient with grade II (A) and grade III (B) glioma. The CBV and CBF maps in (A) show elevated blood volume and blood flow within the tumour (8.16 mL/100 mL², 111 mL/100 g, respectively) compared with the normal WM (4.9 mL/100 mL², 71.4 mL/100 g/min, respectively).

Diffusion and perfusion weighted magnetic resonance imaging methods in non-enhancing gliomas

Short title: Diffusion and perfusion weighted MRI in non-enhancing gliomas

Abstract:

Routine diagnostic magnetic resonance imaging (MRI) utilises enhancement of the tumour tissue as a marker of malignancy in intracranial gliomas. However, several high-grade tumours do not exhibit enhancement and conversely, some low-grade gliomas do demonstrate enhancement. Hence, conventional MRI has a limited role in the accurate grading of gliomas. Advanced MRI methods that evaluate the tissue microstructure and tumour haemodynamics provide a better understanding of tumour biology and promise to provide more accurate grading. These advanced MRI methods include diffusion-weighted imaging (DWI), diffusion tensor imaging (DTI), diffusion-kurtosis imaging (DKI), arterial spin labelling (ASL) imaging, dynamic-susceptibility contrast (DSC) imaging and dynamic contrast-enhanced (DCE) imaging. This review focuses on the utility of these methods for better characterisation and grading of non-enhancing gliomas and discusses how quantitative MRI data can be utilized in these settings.

Introduction:

Primary tumours arising in the central nervous system (CNS) are known as gliomas. The World Health Organisation (WHO) classification system is typically used to classify and grade CNS tumours based primarily on histological features of the tumour tissue, and it was updated in 2016 to include molecular markers as well ^[1, 2]. Typically, gliomas of grades I and II are considered low-grade gliomas (LGGs), while gliomas of grades III and IV are considered high-grade gliomas (HGGs) ^[3] due to the difference in treatment of low- versus high-grade gliomas. However, accurate differentiation of tumour malignancy can only be obtained through stereotactic biopsy or resected tumour tissue, which is associated with morbidity ^[4]. The risk of sampling error and the impact of the neuropathologist's experience on the outcomes are further limitations to this method ^[5].

Conventional MRI is often used for the detection and diagnosis of brain tumours ^[6]. Most clinical brain tumour MRI protocols include T1- and T2-weighted images, fluid-attenuated inversion recovery (FLAIR) images and gadolinium enhanced T1-weighted images (Figure 1). These images help determine the location, size and extent of the tumour ^[7]. Contrast enhancement using gadolinium-based contrast agents is indicative of the breakdown of the blood brain barrier (BBB). Generally, the accumulation of the contrast agent indicates whether the lesion is high-grade (presence) or low-grade (absence) ^[8, 9]. However, malignancy is also exhibited by nearly a third of non-enhancing gliomas, while enhancement is observed in certain LGGs ^[9, 10]. Hence, HGGs and LGGs cannot be definitively distinguished based on contrast enhancement alone ^[11].

In conventional MRI, LGGs appear as a homogenous mass and seldom exhibit peritumoural oedema or contrast enhancement ^[12]. In contrast, HGGs reveal heterogeneous contrast enhancement with regions of necrosis, haemorrhage, extensive peritumoural oedema and cystic regions ^[7]. These features are attributed to the cellular characteristics of HGGs, which include both grade III and IV glial tumours. Grade III tumours are characterised by mitotic and anaplastic cells and are most frequently diagnosed as anaplastic astrocytomas (AAs). On the other hand, grade IV gliomas reveal elevated vascularity and cellularity with enhanced necrotic appearance and are usually labelled as glioblastoma multiforme (GBM). Overall, the imaging features observed in LGGs and HGGs are not specific to a particular grade. In some cases, LGGs may display similar morphological features to HGGs, and the latter may present relatively benign imaging findings ^[13, 14], leading to inaccurate tumour staging. The necessity of accurate grading is exacerbated in non-enhancing gliomas because critical treatment decisions need to be made.

Surgery and chemotherapy represent the preferred treatments for HGGs, while a wait-and-watch approach is generally used to treat LGGs. Therefore, to overcome the shortcomings of conventional MRI, advanced imaging has been employed to enable quantitative analysis and improve the accuracy of diagnosis.

The development of advanced imaging techniques, such as diffusion tensor imaging (DTI) and perfusion MRI, has enabled more sensitive tumour characterisation and grading than conventional MRI ^[4, 13]. These methods provide information about tumour cellularity, proliferation, disruption of white matter, tumour vascularity and vessel permeability ^[14, 15] (summarized in Table 1) and, as such, could allow for improved tumour grading ^[4, 16]. Therefore, the purpose of this review is to examine recent results using diffusion and perfusion methods for tumour characterisation and grading non-enhancing gliomas.

Diffusion techniques:

Diffusion-weighted imaging (DWI) is predominantly used within neuroimaging as well as in oncological applications outside the brain. Standard DWI methods incorporate Einstein's original concept that the diffusion of water molecules follows a Gaussian (normal) distribution ^[17]. Typically, DWI measures random water molecular movement in tissue, and its derived parameter, apparent diffusion coefficient (ADC), represents direction-independent water displacement. DWI can provide information about tissue microstructure without the use of exogenous contrast agents ^[18]. Previous studies using DWI reported a strong association between ADC and cell density ^[18, 19]. It has been shown that within brain tumour tissue (high cellularity), free water motion is restricted and the measured ADC is low, whereas in normal brain tissues, the relatively lower cellularity leads to higher ADC values than those of the tumour ^[20].

The utility of ADC in characterising non-enhancing gliomas has also been investigated. One study reported that ADC values were significantly lower in HGGs compared to LGGs ^[21]. Another study observed lower ADC values in the solid portions of non-enhancing HGGs compared to LGGs ^[22], which suggested that ADC values were useful in differentiating between non-enhancing HGGs and LGGs. However, no significant differences in the ADC values of the peritumoural regions were observed in this study ^[22]. Despite these promising findings, mixed findings have also been reported with regard to the ability of ADC to differentiate LGGs from HGGs. Higher ADC values have been noted in LGGs due to their cellular morphology ^[23, 24], but overlapping ADC values between the two groups have also been reported. One study highlighted the absence of significant differences despite the higher ADC values in LGGs ^[25]. This finding was supported by a second study that reported a lack of significant differences in

ADC values between different glial tumours from either the peritumoural oedema or the solid tumour region ^[26].

The lack of significant differences in ADC values may be due to the simplistic analysis of DWI data using a mono-exponential fitting. The diffusion of water molecules in tumour tissues is much more complicated than in free water due to the complex cellular structures within the tumour microenvironment, which impacts barriers to diffusion. Consequently, the displacement probability of water in tumour tissue may substantially deviate from the conventionally used Gaussian form. Therefore, alternate diffusion models have been proposed to account for the non-Gaussian diffusion behaviour to facilitate a more comprehensive analysis of DWI data ^[17].

Diffusion kurtosis imaging (DKI) is a diffusion imaging technique that does not assume Gaussian distribution of water molecules and measures deviation from Gaussian behaviour. It has been proposed to more accurately characterise the complicated water diffusion in biological tissues. It provides additional information about tumour heterogeneity by measuring kurtosis metrics, including the mean kurtosis (MK), axial kurtosis (AK) and radial kurtosis (RK), as seen in Figure 2 ^[27, 28]. These parameters represent the mean deviation from Gaussianity, the directional deviation from Gaussianity along the axial diffusion direction and the directional deviation perpendicular to the axial diffusion direction ^[29].

A previous study assessed the contribution of DKI parameters, and demonstrated that all DKI parameters were significantly higher in HGGs when contrasted against LGGs ^[30]. The same study reported that these parameters were also significantly different between grades I and II and between grades II and IV ^[30]. Tietze et al. also noted that all DKI exhibited significantly higher values in HGGs compared to LGGs ^[31]. Another study noted that the average MK value was significantly higher in the tumour cores of HGGs compared to those of LGGs ^[32]. However, another study reported that DKI variables did not differ significantly between grades II and III ^[33]. Despite these early promising findings, we are unaware of any studies specifically evaluating the utility of DKI in differentiating non-enhancing gliomas, and hence its role in these gliomas remains speculative.

The complex yet organised structure of the central nervous system (CNS), including myelinated and unmyelinated axons, cellular membrane, and the presence of proteins and intracellular organelles affect water diffusion inside the CNS. These factors could substantially impact the water diffusion pattern in the CNS, which can be broadly classified into isotropic and anisotropic diffusion ^[28]. Therefore, advanced

diffusion models using diffusion tensor imaging (DTI) have been proposed to account for diffusion directionality and the diffusion anisotropy of water in tumour tissue ^[34].

DTI determines the directionality of diffusion and provides additional information on the microstructure of the brain ^[27]. It involves acquisition of diffusion-weighted images in at least six diffusion gradient directions. The motion of water molecules on the X, Y and Z axes is assessed based on a calculation of three diffusion tensor eigenvalues, namely, λ_1 , λ_2 and λ_3 ^[12, 17]. The fractional anisotropy (FA), which measures the tendency of water molecules for diffusion in a particular direction, and the magnitude of diffusion (MD) represent the two most commonly studied DTI parameters. MD is mathematically analogous to the ADC value estimated by conventional DWI experiments. Furthermore, axial diffusion (AD) and radial diffusion (RD) denote the rate of diffusion along the primary diffusion axis and in the transverse direction, respectively, as displayed in Figure 3 ^[35, 36].

FA values have been utilised in the grading of gliomas and in demonstrating tumour infiltration in the normal brain. Various studies have reported the ability of FA to differentiate between different glioma grades ^[37-39]. HGGs demonstrated significantly higher FA values than those in LGGs, with a threshold FA value of 0.188 differentiated between LGGs and HGGs ^[37]. This study also reported a positive relationship between glioma cell density and FA. However, previous research has noted a negative relationship between glioma cell density and FA ^[38, 40]. Another study indicated a lack of significant differences between anaplastic astrocytomas and LGGs ^[41]. Utility of FA in the grading of non-enhancing gliomas has also been evaluated. A previous study suggested a cut-off value of 0.129 to separate HGGs from LGGs, with significantly lower FA values exhibited in LGGs ^[16]. However, another study indicated a lack of significant differences in FA values between LGGs and HGGs from non-enhancing areas of the tumour ^[42]. Yet another study reported no significant differences in FA values between grade II and III non-enhancing gliomas ^[43].

MD reflects directionally averaged diffusivity of water, which is sensitive to oedema, cellularity and necrosis, Table 1 ^[44] and was found to be significantly lower in HGGs compared to LGGs ^[25]. Another study reported that grade I gliomas exhibited significantly higher MD in comparison to grade III and IV gliomas, whilst there was a lack of difference in MD values between grade II and III gliomas ^[37]. With regard to non-enhancing gliomas, Lee et al. demonstrated that even non-enhancing areas of HGGs demonstrated a significantly lower MD compared to LGGs ^[42]. This result was further supported by Liu et

al. however, their findings did not reach statistical significance ^[16]. On the other hand, another study reported no significant differences in MD values between grade II and III non-enhancing gliomas ^[43].

Several studies have suggested that axonal integrity/degeneration can be identified through AD, while myelin damage can be identified with RD ^[45, 46]. Published studies suggest that AD and RD were capable of differentiating between HGGs and LGGs ^[25, 43]. Yuan et al. ^[47] reported that the RD and AD values were significantly higher in LGGs than in HGGs. Another study noted that LGGs exhibited significantly higher RD and AD values when contrasted against HGGs, and this result considered differences between gliomas grades II and III and between grades II and IV ^[25]. In regard to non-enhancing gliomas, one study reported no significant differences in AD and RD between grade II and III gliomas ^[43].

To conclude the findings of diffusion imaging, even though some evidence suggests that these methods are useful in assessing tissue microstructure and heterogeneity in brain tumours, none of the diffusion parameters in isolation have been suggested to conclusively differentiate between non-enhancing LGGs and HGGs. However, we believe that by combining the information from the most commonly used DTI parameters, MD and FA, with conventional imaging as well as perfusion imaging (as discussed below) might aid in the accurate grading of non-enhancing gliomas. Besides having a heterogeneous structural microenvironment, brain tumours are also known to have a complex and heterogeneous vasculature, relying on angiogenesis to maintain an adequate blood supply. MRI-based perfusion imaging methods can provide information about tumour vasculature and thus may be able to aid in accurate tumour grading.

Perfusion techniques:

Perfusion MRI methods provide estimates of how well a tissue is supplied with blood. Perfusion MRI can be broadly classified into two methods: one that uses an endogenous contrast agent (water) to measure blood flow and another that uses an exogenous contrast agent, typically gadolinium-based contrast agents (GBCA), to study contrast kinetics. The first method is generally referred to as arterial spin labelling (ASL), which is a completely non-invasive MRI technique that measures blood flow by using magnetically labelled water protons in arterial blood as an endogenous tracer ^[48]. The parameter most commonly derived from ASL methods is cerebral blood flow (CBF). The relative rCBF has been used to discriminate between low- and high-grade gliomas. Some studies suggest that HGGs demonstrate significantly higher rCBF values than those in LGGs ^[49, 50]. Another study reported a strong correlation

between ASL-derived CBF values and dynamic susceptibility contrast (DSC)-derived CBF values in brain tumours^[51]. However, one study found that the correlation between DSC-derived rCBF and ASL-derived rCBF was weaker^[49]. To our knowledge, the use of ASL in evaluating non-enhancing gliomas has not been investigated.

Whilst ASL has the advantage of being completely non-invasive, it suffers from low signal-to-noise ratio as well as sensitivity to motion since it is a difference method in which ‘labelled’ images are subtracted from ‘control’ images^[52]. The more commonly used perfusion imaging method uses an exogenous contrast agent and can either be performed using dynamic contrast enhanced (DCE) or dynamic susceptibility contrast (DSC) enhanced imaging. DCE imaging relies on the acquisition of T1-weighted images and this method detects changes in MR signal as the contrast agent passes through the blood vessels and leaks into the interstitial space during the BBB breakdown. Hence, the images obtained through this method can be indicative of microvascular properties such as vascular permeability and flow and are indicated by the parameter K^{trans} ^[53]. DCE-MRI has been evaluated to discriminate between gliomas of different grades. The K^{trans} parameter can be used to quantify the permeability of tumour vessels, as shown in Figure 4^[54]. This study reported that the skewness of K^{trans} was superior in differentiating between grade II and grade III gliomas^[55]. In addition, significantly higher K^{trans} was reported in HGGs compared to LGGs^[54, 56–58]. It should be noted that K^{trans} reflects a combination of microvascular blood flow, vessel permeability and vessel density. These factors are correlated with the distribution of tumour vessels and abnormal permeability^[59, 60], indicating that contrast agents permeate more easily in HGGs than in LGGs. To our knowledge, DCE-MRI studies have not been reported in non-enhancing gliomas.

In DSC imaging, haemodynamic parameters are measured by studying the changes in MR intensity during the initial passage of the paramagnetic contrast agent^[28, 61]. The cerebral blood volume (CBV), cerebral blood flow (CBF) and mean transit time (MTT) constitute the main hemodynamic parameters associated with DSC-MRI. Indicative of the blood supply of a particular region of tissue at a particular moment, the CBV can be derived from the area under the fitted curve. Meanwhile, the CBV-to-MTT ratio reflects CBF. As the change in signal intensity and the gadolinium concentration is not linearly correlated, it is challenging to quantitatively measure these parameters. Hence, they are typically normalised to the contralateral white matter and the values are represented as ‘relative’ (rCBV, rCBF and rMTT), as depicted in Figure 5^[62, 63]. DSC has been shown to differentiate between LGGs and HGGs. Some studies have reported that rCBV values aid in differentiation between various glioma grades by recognising histopathological features, including vascularisation and the degree of angiogenesis, Table 1^[64, 65]. The

rCBV values of LGGs were negligible or very low, indicating minimal vascularisation when contrasted against HGGs. Anaplastic astrocytomas demonstrated higher rCBV values compared to LGGs, but these values were lower than in GBMs, the latter representing gliomas with the greatest level of hypervascularisation. Several studies have also reported variation in the degree of vascularisation of LGGs and HGGs ^[16, 66-69]. Despite the range of rCBV values reported in the literature amongst various types of gliomas, the commonality was the observation of higher rCBV in gliomas, which was likely due to the associated micro-vascular density noted in each grade. It is important to realise that gliomas constitute a heterogeneous range of tumours and overlap in rCBV values should be expected. For example, even low-grade oligodendrogliomas have been noted to have higher angiogenesis, which correlated with higher rCBV values than typically reported in HGGs ^[16, 70, 71].

Utilising DSC derived parameters to differentiate between non-enhancing LGGs and HGGs has led to ambiguous findings. Liu et al. reported a lack of significant differences in rCBV ratios between LGGs and HGGs ^[16], whereas, Fan et al. noted significantly higher rCBV values in non-enhancing areas of HGGs than in LGGs ^[72]. The latter study also noted significant variation in rCBV values in peritumoural regions ^[72]. This was supported by a study that reported statistically higher rCBV_{max} ratios for grade III astrocytomas compared to grade I or grade II astrocytomas ^[11]. However, previous studies also demonstrated no significant differences in rCBV_{max} between grade II and III non-enhancing gliomas ^[43, 73].

With regard to the utility of MTT and DSC-derived rCBF values in non-enhancing gliomas, one study reported significant differences in rCBF and rMTT between grade II and GBM ^[43]. However, in the same study, no significant differences in rCBF and rMTT were noted between grade II and grade III non-enhancing gliomas ^[43]. Another study reported significant differences in rCBF values between these two grades of gliomas ^[74]. This finding was further supported by a study that reported higher rCBF values associated with grades of gliomas, with significant variation identified between LGGs and HGGs ^[67].

Despite the observed variability in results, which may in part be due to a small sample size, methodological differences or the inclusion of different histological sub-types of gliomas, it is generally accepted that rCBV provides a rigorous means of assessing gliomas, thereby allowing it to act as a potential imaging marker of malignancy and degree of tumour angiogenesis, at least for enhancing tumours.

We acknowledge that the current literature, with mixed results about the utility of diffusion and perfusion imaging in non-enhancing gliomas is still emerging, but we believe that the data is not contradictory in the sense that opposing values (higher or lower between HGG and LGG) are not reported for any particular parameter. As the trends are generally similar between different studies, we believe that the apparent discrepancy is primarily due to differences in data analysis or in choice of experimental groups (including astrocytomas and oligodendrogliomas together, for example) rather than the underlying insensitivity of the diffusion or perfusion imaging based parameter. We therefore recommend a standard set of imaging and analysis parameters evaluated in a homogenous histological subgroup, to be used in a multi-centre prospective trial to establish the role of these parameters in non-enhancing gliomas. In addition, a decision-making tool/algorithm combining the various imaging parameters is highly desirable for a better diagnosis of non-enhancing gliomas in the clinical practise. This could use simplistic statistical methods such a logistic regression analyses to find the best combination of imaging parameters or use more sophisticated image analysis methods such as machine learning, artificial neural networks, artificial intelligence or deep learning methods ^[75-77].

Conclusion:

Both diffusion and perfusion imaging methods continue to aid in the accurate diagnosis of brain tumours; however, their role in assessing non-enhancing gliomas is still in its infancy, and the few early promising reports need to be validated in a large cohort of patients, preferably studied using a standardised, multi-center imaging trial.

References:

1. Louis, D.N., et al., *The 2007 WHO classification of tumours of the central nervous system*. Acta Neuropathologica, 2007. 114(5): p. 547-547 DOI: 10.1007/s00401-007-0278-6.
2. Raizer, J. and A. Parsa, *Current understanding and treatment of gliomas*. Vol. 163. 2015: Springer.
3. Wesseling, P. and D. Capper, *WHO 2016 Classification of gliomas*. Neuropathol Appl Neurobiol, 2018. 44(2): p. 139-150 DOI: 10.1111/nan.12432.
4. Guzman-De-Villoria, J.A., et al., *Added value of advanced over conventional magnetic resonance imaging in grading gliomas and other primary brain tumors*. Cancer Imaging, 2014. 14(1): p. 35 DOI: 10.1186/s40644-014-0035-8.
5. Muragaki, Y., et al., *Low-grade glioma on stereotactic biopsy: how often is the diagnosis accurate?* Min-minimally invasive Neurosurgery, 2008. 51(05): p. 275-279 DOI: 10.1055/s-0028-1082322
6. Herberholz, J., et al., *Non-invasive imaging of neuroanatomical structures and neural activation with high-resolution MRI*. Front Behav Neurosci, 2011. 5: p. 16 DOI: 10.3389/fnbeh.2011.00016.
7. Villanueva-Meyer, J.E., M.C. Mabray, and S. Cha, *Current Clinical Brain Tumor Imaging*. Neurosurgery, 2017. 81(3): p. 397-415 DOI: 10.1093/neuros/nyx103.
8. Mabray, M.C., R.F. Barajas, Jr., and S. Cha, *Modern brain tumor imaging*. Brain Tumor Res Treat, 2015. 3(1): p. 8-23 DOI: 10.14791/btrt.2015.3.1.8.
9. Scott, J.N., et al., *How often are nonenhancing supratentorial gliomas malignant? A population study*, Neurology, 2002. 59(6): p. 947-949 DOI: 10.1212/WNL.59.6.947.
10. Upadhyay, N. and A.D. Waldman, *Conventional MRI evaluation of gliomas*. Br J Radiol, 2011. 84 Spec No 2: p. S107-11 DOI: 10.1259/bjr/65711810.
11. Morita, N., et al., *Dynamic susceptibility contrast perfusion weighted imaging in grading of nonenhancing astrocytomas*. Journal of Magnetic Resonance Imaging, 2010. 32(4), pp.803-808 DOI: 10.1002/jmri.22324.
12. Guillevin, R., et al., *Low-grade gliomas: the challenges of imaging*. Diagn Interv Imaging, 2014. 95(10): p. 957-63 DOI: 10.1016/j.diii.2014.07.005.
13. Drake-Perez, M., et al., *Clinical applications of diffusion weighted imaging in neuroradiology*. Insights Imaging, 2018. 9(4): p. 535-547 DOI: 10.1007/s13244-018-0624-3.
14. Young, G.S., *Advanced MRI of adult brain tumors*. Neurol Clin, 2007. 25(4): p. 947-73, viii DOI: 10.1016/j.ncl.2007.07.010.
15. Saini, J., et al., *Comparative evaluation of cerebral gliomas using rCBV measurements during sequential acquisition of T1-perfusion and T2*-perfusion MRI*. PLoS One, 2019. 14(4): p. e0215400. DOI: 10.1371/journal.pone.0215400.
16. Liu, X., et al., *MR diffusion tensor and perfusion-weighted imaging in preoperative grading of supratentorial nonenhancing gliomas*. Neuro Oncol, 2011. 13(4): p. 447-55 DOI: 10.1093/neuonc/noq197.
17. Yuan, J., et al., *Non-Gaussian Analysis of Diffusion Weighted Imaging in Head and Neck at 3T: A Pilot Study in Patients with Nasopharyngeal Carcinoma*. PLoS One, 2014. 9(1): p. e87024. DOI: 10.1371/journal.pone.0087024.
18. Harkins, K.D., et al., *Assessment of the effects of cellular tissue properties on ADC measurements by numerical simulation of water diffusion*. Magn Reson Med, 2009. 62(6): p. 1414-22 DOI: 10.1002/mrm.22155.
19. Surov, A., H.J. Meyer, and A. Wienke, *Correlation between apparent diffusion coefficient (ADC) and cellularity is different in several tumors: a meta-analysis*. Oncotarget. 2017. 8(35): p. 59492-59499 DOI:10.18632/oncotarget.17752.

20. Bulakbasi, N. and Y. Paksoy, *Advanced imaging in adult diffusely infiltrating low-grade gliomas*. Insights Imaging, 2019. 10(1): p. 122 DOI: 10.1186/s13244-019-0793-8.
21. Hu, Y.-C., et al., *Comparison between ultra-high and conventional mono b-value DWI for preoperative glioma grading*. Oncotarget, 2017. 8(23): p. 37884-37895 DOI:10.18632/oncotarget.14180.
22. Fan, G.G., et al., *Usefulness of diffusion/perfusion-weighted MRI in patients with non-enhancing supratentorial brain gliomas: a valuable tool to predict tumour grading?* Br J Radiol, 2006. 79(944): p. 652-8 DOI: 10.1259/bjr/25349497.
23. Yamasaki, F., et al., *Apparent diffusion coefficient of human brain tumors at MR imaging*. Radiology, 2005. 235(3): p. 985-991 DOI: 10.1148/radiol.2353031338.
24. Svolos, P., et al., *Investigating brain tumor differentiation with diffusion and perfusion metrics at 3T MRI using pattern recognition techniques*. Magn Reson Imaging, 2013. 31(9): p. 1567-77 DOI: 10.1016/j.mri.2013.06.010.
25. Server, A., et al., *Analysis of diffusion tensor imaging metrics for gliomas grading at 3 T*. Eur J Radiol, 2014. 83(3): p. e156-65 DOI: 10.1016/j.ejrad.2013.12.023.
26. Rizzo, L., et al., *Role of diffusion- and perfusion-weighted MR imaging for brain tumour characterisation*. Radiol Med, 2009. 114(4): p. 645-59 DOI: 10.1007/s11547-009-0401-y.
27. Steven, A.J., J. Zhuo, and E.R. Melhem, *Diffusion kurtosis imaging: an emerging technique for evaluating the microstructural environment of the brain*. AJR Am J Roentgenol, 2014. 202(1): p. W26-33 DOI: 10.2214/AJR.13.11365.
28. Arab, A., et al., *Principles of diffusion kurtosis imaging and its role in early diagnosis of neurodegenerative disorders*. Brain Res Bull, 2018. 139: p. 91-98 DOI: 10.1016/j.brainresbull.2018.01.015.
29. Wang, S., et al., *Empirical comparison of diffusion kurtosis imaging and diffusion basis spectrum imaging using the same acquisition in healthy young adults*. Frontiers in neurology, 2017. 8: p. 118 DOI:10.3389/fneur.2017.00118.
30. Andersson, J.L.R. and S.N. Sotiropoulos, *An integrated approach to correction for off-resonance effects and subject movement in diffusion MR imaging*. Neuroimage, 2016. 125: p. 1063-1078 DOI: 10.1016/j.neuroimage.2015.10.019.
31. Tietze, A., et al., *Mean Diffusional Kurtosis in Patients with Glioma: Initial Results with a Fast Imaging Method in a Clinical Setting*. AJNR Am J Neuroradiol, 2015. 36(8): p. 1472-8 DOI: 10.3174/ajnr.A4311.
32. Raab, P., et al., *Cerebral gliomas: diffusional kurtosis imaging analysis of microstructural differences*. Radiology, 2010. 254(3): p. 876-81 DOI: 10.1148/radiol.09090819.
33. Delgado, A.F., et al., *Diffusion Kurtosis Imaging of Gliomas Grades II and III - A Study of Perilesional Tumor Infiltration, Tumor Grades and Subtypes at Clinical Presentation*. Radiol Oncol, 2017. 51(2): p. 121-129 DOI: 10.1515/raon-2017-0010.
34. Dubey, A., R. Kataria, and V.D. Sinha, *Role of Diffusion Tensor Imaging in Brain Tumor Surgery*. Asian J Neurosurg, 2018. 13(2): p. 302-306 DOI: 10.4103/ajns.AJNS_226_16.
35. Zeestraten, E.A., et al., *Application of Diffusion Tensor Imaging Parameters to Detect Change in Longitudinal Studies in Cerebral Small Vessel Disease*. PLoS One, 2016. 11(1): p. e0147836 DOI: 10.1371/journal.pone.0147836.
36. Abdullah, K.G., et al., *Use of diffusion tensor imaging in glioma resection*. Neurosurgical focus, 2013. 34(4), p.E1 DOI: 10.3171/2013.1.FOCUS12412.
37. Inoue, T., et al., *Diffusion tensor imaging for preoperative evaluation of tumor grade in gliomas*. Clin Neurol Neurosurg, 2005. 107(3): p. 174-80 DOI: 10.1016/j.clineuro.2004.06.011.
38. El-Serougy, L., et al., *Assessment of diffusion tensor imaging metrics in differentiating low-grade from high-grade gliomas*. Neuroradiol J, 2016. 29(5): p. 400-7 DOI: 10.1177/1971400916665382.

39. Jiang, R., et al., *The value of diffusion tensor imaging in differentiating high-grade gliomas from brain metastases: a systematic review and meta-analysis*. PLoS One, 2014. 9(11): p. e112550 DOI: 10.1371/journal.pone.0112550.
40. Stadlbauer, A., et al., *Gliomas: histopathologic evaluation of changes in directionality and magnitude of water diffusion at diffusion-tensor MR imaging*. Radiology, 2006. 240(3): p. 803-810 DOI: 10.1148/radiol.2403050937.
41. Goebell, E., et al., *Low-grade and anaplastic gliomas: differences in architecture evaluated with diffusion-tensor MR imaging*. Radiology, 2006. 239(1): p. 217-22 DOI: 10.1148/radiol.2383050059.
42. Lee, H.Y., et al., *Diffusion-tensor imaging for glioma grading at 3-T magnetic resonance imaging: analysis of fractional anisotropy and mean diffusivity*. Journal of computer assisted tomography, 2008. 32(2): p. 298-303 DOI: 10.1097/RCT.0b013e318076b44d.
43. Alkanhal, H., et al., *Evaluating the role of Diffusion Tensor Imaging and Dynamic Susceptibility Contrast perfusion imaging in the diagnosis of non-enhancing brain tumours*. 2020, University of liverpool: Liverpool.
44. Alexander, A.L., et al., *Diffusion tensor imaging of the brain*. Neurotherapeutics, 2007. 4(3): p. 316-29 DOI: 10.1016/j.nurt.2007.05.011.
45. Zhu, F.P., et al., *Clinical application of motor pathway mapping using diffusion tensor imaging tractography and intraoperative direct subcortical stimulation in cerebral glioma surgery: a prospective cohort study*. Neurosurgery, 2012. 71(6): p. 1170-83; discussion 1183-4 DOI: 10.1227/NEU.0b013e318271bc61.
46. Rajagopalan, V., et al., *A Basic Introduction to Diffusion Tensor Imaging Mathematics and Image Processing Steps*. Brain Disord Ther, 2017. 6(229): p. 2 DOI: 10.4172/2168-975X.1000229.
47. Yuan, W., et al., *Characterization of abnormal diffusion properties of supratentorial brain tumors: a preliminary diffusion tensor imaging study*. J Neurosurg Pediatr, 2008. 1(4): p. 263-9 DOI: 10.3171/PED/2008/1/4/263.
48. Haller, S., et al., *Arterial Spin Labeling Perfusion of the Brain: Emerging Clinical Applications*. Radiology, 2016. 281(2): p. 337-356 DOI: 10.1148/radiol.2016150789.
49. Cebeci, H., et al., *Assesment of perfusion in glial tumors with arterial spin labeling; comparison with dynamic susceptibility contrast method*. European Journal of Radiology, 2014. 83(10): p. 1914-1919 DOI: 10.1016/j.ejrad.2014.07.002.
50. Kong, L., et al., *A meta-analysis of arterial spin labelling perfusion values for the prediction of glioma grade*. Clinical Radiology, 2017. 72(3): p. 255-261 DOI: 10.1016/j.crad.2016.10.016.
51. Arisawa, A., et al., *Comparative study of pulsed-continuous arterial spin labeling and dynamic susceptibility contrast imaging by histogram analysis in evaluation of glial tumors*. Neuroradiology, 2018. 60(6): p. 599-608 DOI: 10.1007/s00234-018-2024-2.
52. Ferré, J.C., et al., *Arterial spin labeling (ASL) perfusion: Techniques and clinical use*. Diagnostic and Interventional Imaging, 2013. 94(12): p. 1211-1223 DOI: 10.1016/j.diii.2013.06.010.
53. Pope, W.B. and G. Brandal, *Conventional and advanced magnetic resonance imaging in patients with high-grade glioma*. Q J Nucl Med Mol Imaging, 2018. 62(3): p. 239 -253 DOI:10.23736/S1824-4785.18.03086-8.
54. Lacerda, S. and M. Law, *Magnetic resonance perfusion and permeability imaging in brain tumors*. Neuroimaging Clin N Am, 2009. 19(4): p. 527-57 DOI: 10.1016/j.nic.2009.08.007.
55. Falk, A., et al., *Discrimination between glioma grades II and III in suspected low-grade gliomas using dynamic contrast-enhanced and dynamic susceptibility contrast perfusion MR imaging: a histogram analysis approach*. Neuroradiology, 2014. 56(12): p. 1031-8 DOI: 10.1007/s00234-014-1426-z.
56. Zhao, J., et al., *Quantitative Evaluation of Diffusion and Dynamic Contrast-Enhanced MR in Tumor Parenchyma and Peritumoral Area for Distinction of Brain Tumors*. PLoS ONE, 2015. 10(9): p. 1-15 DOI: 10.1371/journal.pone.0138573.

57. Thompson, G., et al., *Imaging of brain tumors: perfusion/permeability*. Neuroimaging Clin N Am, 2010. 20(3): p. 337-53 DOI: 10.1016/j.nic.2010.04.008.
58. Jia, Z., et al., *Quantitative analysis of neovascular permeability in glioma by dynamic contrast-enhanced MR imaging*. J Clin Neurosci, 2012. 19(6): p. 820-3 DOI: 10.1016/j.jocn.2011.08.030.
59. Bulnes, S., J. Bilbao, and J.V. Lafuente, *Microvascular adaptive changes in experimental endogenous brain gliomas*. Histol Histopathol, 2009. 24(6): p. 693-706 DOI: 10.14670/HH-24.693.
60. Morabito, R., et al., *DCE and DSC perfusion MRI diagnostic accuracy in the follow-up of primary and metastatic intra-axial brain tumors treated by radiosurgery with cyberknife*. Radiat Oncol, 2019. 14(1): p. 65 DOI: 10.1186/s13014-019-1271-7.
61. Calamante, F., *Perfusion magnetic resonance imaging quantification in the brain*, in *Visualization Techniques*. Korean J Radiol, 2014. 15(5): p. 554-577. DOI:10.3348/kjr.2014.15.5.554.
62. Calamante, F., *Perfusion MRI using dynamic-susceptibility contrast MRI: quantification issues in patient studies*. Topics in Magnetic Resonance Imaging, 2010. 21(2): p. 75-85 DOI: 10.1097/RMR.0b013e31821e53f5.
63. Price, S.J., *The role of advanced MR imaging in understanding brain tumour pathology*. Br J Neurosurg, 2007. 21(6): p. 562-75 DOI: 10.1080/02688690701700935.
64. Essig, M., et al., *Perfusion MRI: the five most frequently asked technical questions*. American Journal of Roentgenology, 2013. 200(1): p. 24-34 DOI:10.2214/AJR.12.9543.
65. Fussell, D. and R.J. Young, *Role of MRI perfusion in improving the treatment of brain tumors*. Imaging in Medicine, 2013. 5(5): p. 407-426 DOI: 10.2217/iim.13.50.
66. Geneidi, E.A.S.H., et al., *Potential role of quantitative MRI assessment in differentiating high from low-grade gliomas*. The Egyptian Journal of Radiology and Nuclear Medicine, 2016. 47(1): p. 243-253 DOI: 10.1016/j.ejrn.2015.11.005.
67. Ma, H., et al., *Three-dimensional arterial spin labeling imaging and dynamic susceptibility contrast perfusion-weighted imaging value in diagnosing glioma grade prior to surgery*. Exp Ther Med, 2017. 13(6): p. 2691-2698 DOI: 10.3892/etm.2017.4370.
68. Xu, W., et al., *The performance of MR perfusion-weighted imaging for the differentiation of high-grade glioma from primary central nervous system lymphoma: A systematic review and meta-analysis*. PLoS One, 2017. 12(3): p. e0173430 DOI: 10.1371/journal.pone.0173430.
69. Abrigo, J.M., et al., *Magnetic resonance perfusion for differentiating low-grade from high-grade gliomas at first presentation*. Cochrane Database Syst Rev, 2018. 1(1): p. CD011551 DOI: 10.1002/14651858.CD011551.pub2.
70. Cha, S., et al., *Differentiation of low-grade oligodendrogliomas from low-grade astrocytomas by using quantitative blood-volume measurements derived from dynamic susceptibility contrast-enhanced MR imaging*. American journal of neuroradiology, 2005. 26(2): p. 266-273 PMID: 15709123.
71. Xu, M., et al., *Comparison of magnetic resonance spectroscopy and perfusion-weighted imaging in presurgical grading of oligodendroglial tumors*. Neurosurgery, 2005. 56(5): p. 919-26 PMID: 15854239.
72. Fan, G.G., et al., *Usefulness of diffusion/perfusion-weighted MRI in patients with non-enhancing supratentorial brain gliomas: a valuable tool to predict tumour grading?*. BRIT INSTITUTE OF RADIOLOGY, 2006. 79(944): p. 652-8 DOI: 10.1259/bjr/25349497.
73. Sahin, N., et al., *Advanced MR imaging techniques in the evaluation of nonenhancing gliomas: perfusion-weighted imaging compared with proton magnetic resonance spectroscopy and tumor grade*. Neuroradiol J, 2013. 26(5): p. 531-41 DOI: 10.1177/197140091302600506.
74. Hakyemez, B., et al., *High-grade and low-grade gliomas: differentiation by using perfusion MR imaging*. Clin Radiol, 2005. 60(4): p. 493-502 DOI: 10.1016/j.crad.2004.09.009.

75. Booth, T. *et al.*, *Machine learning and glioma imaging biomarkers*. Clinical radiology, 2019. 75(1), p. 20-32 DOI: 10.1016/j.crad.2019.07.001.
76. Kim M, Jung SY, Park JE, et al., *Diffusion- and perfusion-weighted MRI radiomics model may predict isocitrate dehydrogenase (IDH) mutation and tumor aggressiveness in diffuse lower grade glioma*. Eur Radiol, 2020. 30(4). P. 2142-2151 DOI:10.1007/s00330-019-06548-3.
77. Shoaib Y., et al., *Role of Diffusion and Perfusion Magnetic Resonance Imaging in Predicting the Histopathological Grade of Gliomas - A Prospective Study*. Asian J Neurosurg, 2019. 14(1): p. 47-51. DOI: 10.4103/ajns.AJNS_191_16.

Figure legends:

Figure 1: MR images of a patient with a grade III anaplastic astrocytoma who underwent conventional diagnostic MRI. (A) axial T1-weighted pre-contrast, (B) T2 and (C) T1 post-contrast images. No contrast agent enhancement was observed in this patient.

Figure 2: Representative diffusion kurtosis images from a patient with an oligodendroglioma grade II in the right frontal lobe. (A) axial kurtosis, (B) axial diffusivity and (C) radial kurtosis [33].

Figure 3: Representative DTI-derived parametric maps from a patient with a grade II astrocytoma. In FA, the white matter (WM) appears hyper-intense, while the cerebrospinal fluid (CSF) and the tumour appear hypo-intense. In contrast, in MD, AD and RD, the CSF and the tumour are hyper-intense, while the WM appears hypo-intense.

Figure 4: Follow-up MRI of a left frontal primary GBM treated by surgery and stereotactic radiosurgery (SRS). (A) axial contrast-enhanced T1-weighted image demonstrating the enhancing tumour in the frontal lobe, (B) The relative cerebral blood volume rCBV colorimetric map overlaid on the MR image and (C) pixel-by-pixel K^{trans} colorimetric map showing heterogeneous K^{trans} values from the tumour [60].

Figure 5: DSC maps showing the tumour (arrow) from a patient with grade II (A) and grade III (B) glioma. The CBV and CBF maps in (A) show elevated blood volume and blood flow within the tumour (8.16 mL/100 mL², 111 mL/100 g, respectively) compared with the normal WM (4.9 mL/100 mL², 71.4 mL/100 g/min, respectively).

Table 1: Summary of diffusion and perfusion imaging parameters, there physiological interpretation in tumours and their general trends in high (HGG) versus low grade gliomas (LGG).

Parameter	Reflect	Values in HGG [16,37,42,47,54, 74]	Values in LGG
FA	Microstructure integrity	Higher	Lower
MD	Oedema, cellularity and necrosis	Lower	Higher
AD	Axonal integrity/degeneration	Higher	Lower
RD	Myelin damage	Higher	Lower
rCBV	Degree of angiogenesis	Higher	Lower
rCBF	Degree of blood flow	Higher	Lower
K ^{trans}	Vascular Permeability and blood flow	Higher	Lower
rMTT	Vascular Permeability.	Lower	Higher

FA= fractional anisotropy, MD = mean diffusivity, AD = axial diffusivity, RD = radial diffusivity, rCBV = relative cerebral blood volume, rCBF = relative cerebral blood flow, K^{trans} = rate constant of the contrast agent from vascular to insterstitial compartment, rMTT = relative mean transit time of the contrast agent from the vascular to the interstitial compartment. Numbers within brackets indicate the references for the source of these findings.

Figure 1
[Click here to download high resolution image](#)

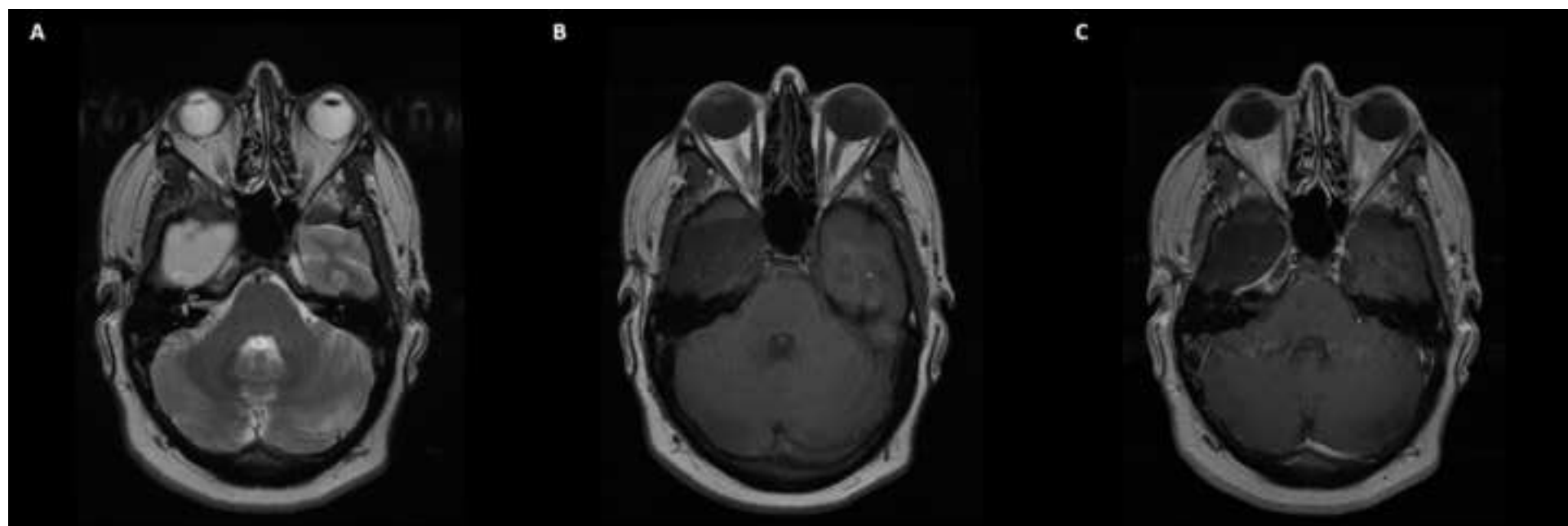


Figure 2
[Click here to download high resolution image](#)

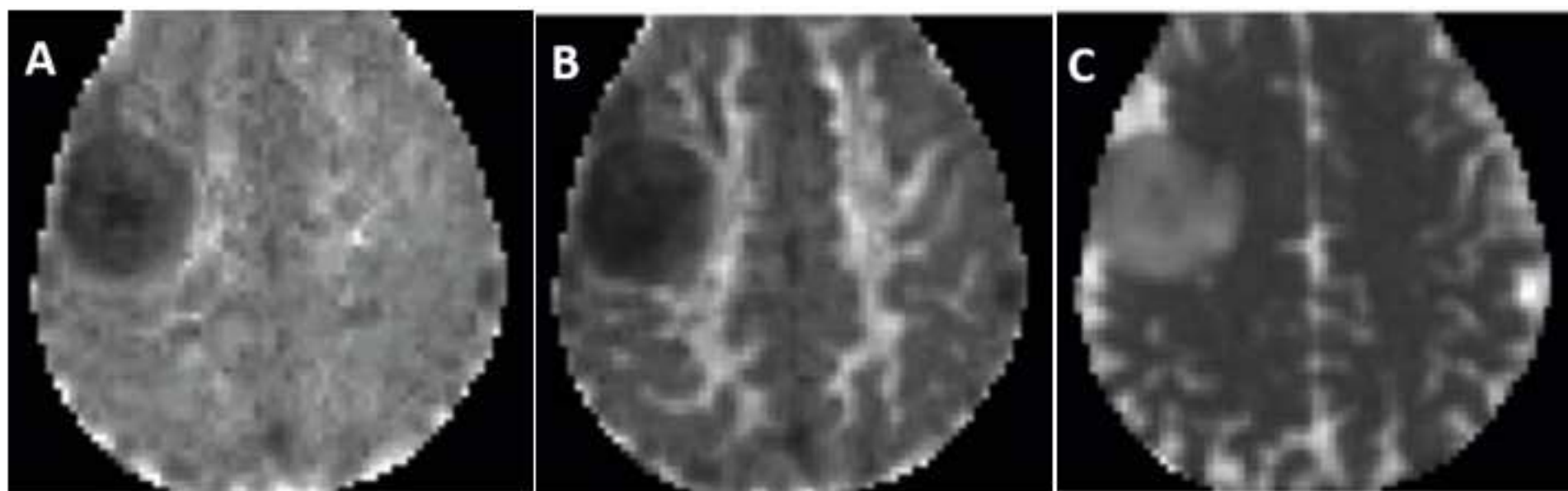


Figure 3
[Click here to download high resolution image](#)

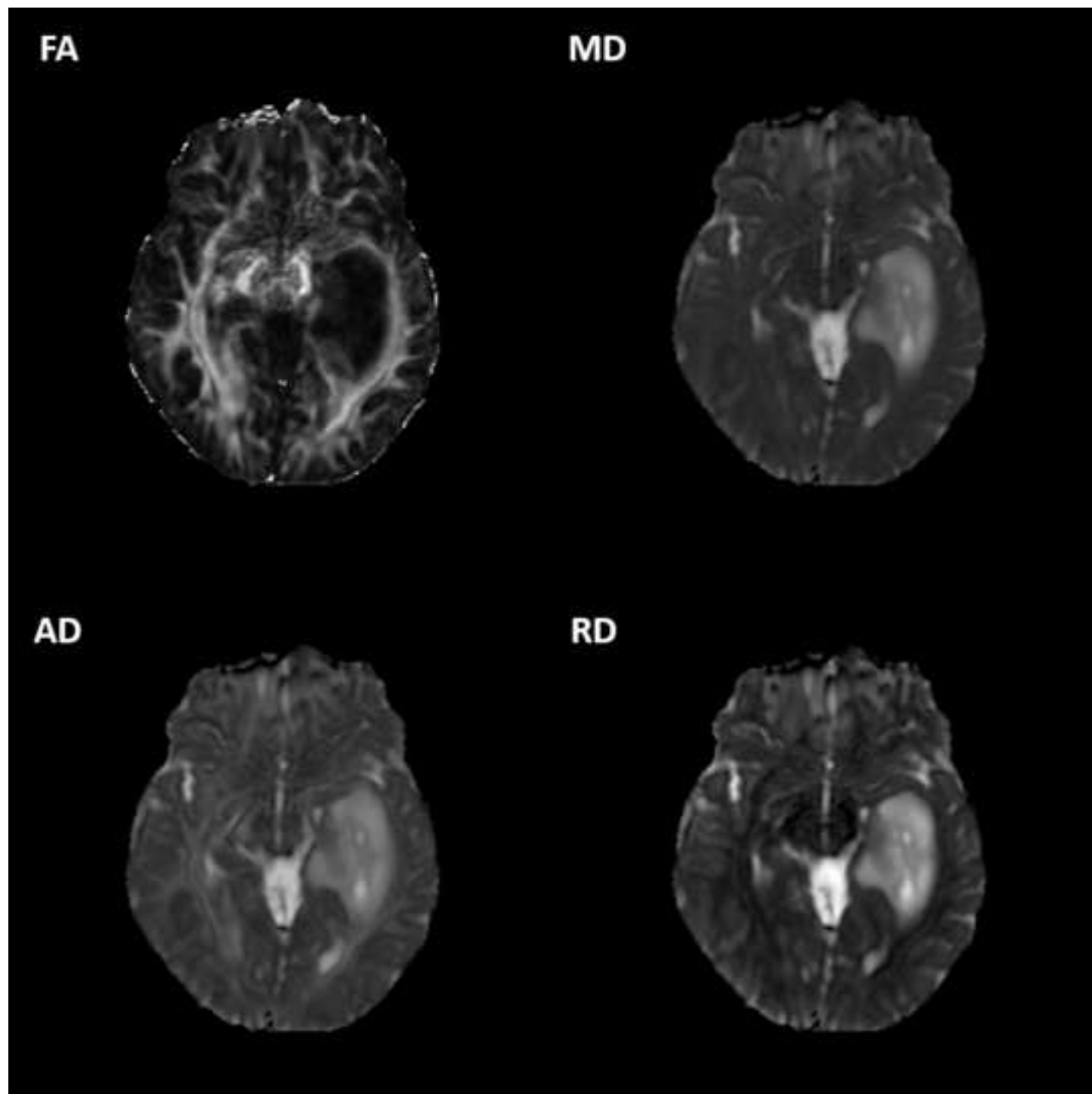


Figure 4
[Click here to download high resolution image](#)

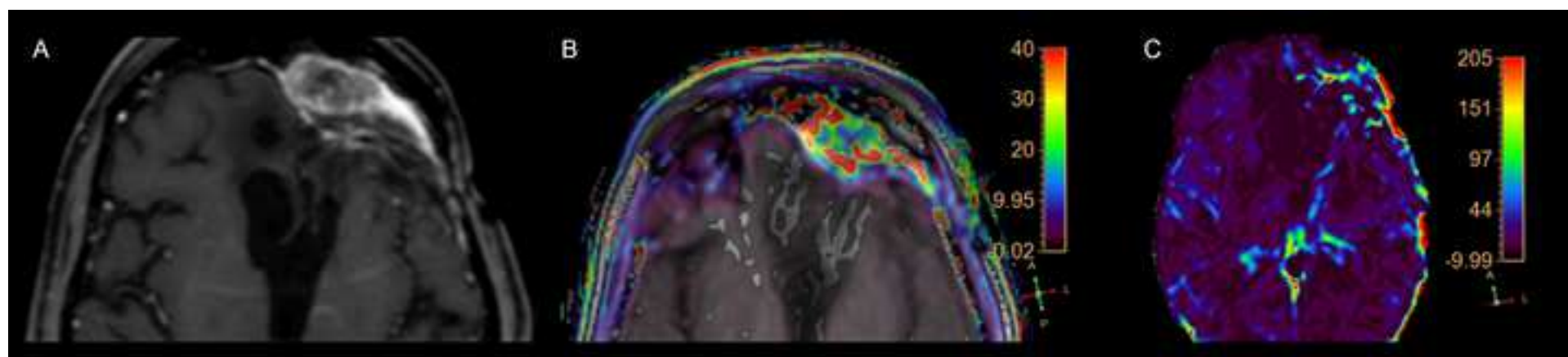


Figure 5
[Click here to download high resolution image](#)

